Contrasting upper atmospheric response to cyclones in the north Indian Ocean during the pre-monsoon and the post-monsoon seasons

Vineet Kumar Singh[1,2,3], **M.K. Roxy**[1] **and Medha Deshpande**[1]

[1] Indian Institute of Tropical Meteorology, Ministry of Earth Sciences, Pune, India

[2] Department of Atmospheric and Space Sciences, Savitribai Phule Pune University, Pune, India

[3] Typhoon Research Center, Jeju National University, Jeju, South Korea

Corresponding author: Vineet Kumar Singh (vineetsingh.jrf@tropmet.res.in)

ORCID: 0000-0002-2932-8523

Key Points

1. Cyclones induce upper-atmosphere warming of 3–4°C during the pre-monsoon season and 1°C during the post-monsoon season.
2. Large heat flux coupled with a strong updraft during pre-monsoon season leads to the difference in the atmospheric response in two seasons.
3. Difference in flux in two seasons is due to the difference in SSTs, wind forcing, and moisture disequilibrium between ocean and atmosphere.

Abstract

Cyclones in the north Indian Ocean evolve differently during the pre-monsoon (April-June) and post-monsoon (October-December) seasons. While several studies have investigated the near-surface ocean-atmospheric interactions, there is a lack of understanding of the upper-atmospheric response during cyclones. In the current study, we find that cyclones in this basin induce warming of 3–4°C at the upper tropospheric levels (300–400 hPa) during the pre-monsoon season, for the period 1982–2019. However, during the post-monsoon season, the upper-level warming is only ~1°C. The contrasting atmospheric response to cyclones in the two seasons is attributed to the contrasting ocean-cyclone-atmosphere coupled interaction. In the pre-monsoon season, higher SSTs coupled with higher wind forcing and moisture disequilibrium enhance the latent heat flux from the ocean to the atmosphere during the cyclones. This enhances convection resulting in enhanced latent heat release and anomalous upper-level warming in the atmosphere. During the post-monsoon season, the SSTs are cooler, and wind forcing and moisture disequilibrium is less than in the pre-monsoon season. As a result, the latent heat flux exchange is weak, leading to weaker convection, reduced latent heat release and weak upper-level warming. The lower atmospheric response to cyclones is also different in the two seasons, with enhanced

evaporative cooling due to a drier lower atmosphere in the pre-monsoon season as compared to the post-monsoon season. Since the Indian Ocean is warming rapidly, it is essential to closely monitor the atmospheric temperature changes accompanying the cyclones in this basin since they can potentially influence largescale atmospheric dynamics and circulation.

Keywords: cyclones, north Indian Ocean, ocean-cyclone-atmosphere interaction, upper atmospheric response, Arabian Sea, Bay of Bengal

1. Introduction

Sea surface temperatures (SSTs) play a dominant role in fueling tropical cyclones worldwide. SSTs are crucial in determining the maximum potential intensity a cyclone can reach during its lifetime (Demaria & Kaplan, 1994). The ocean fuels the cyclones by providing energy through the exchange of enthalpy fluxes between the ocean and the atmosphere (Emanuel, 1986; Ooyama, 1969). This enthalpy flux transfer from the ocean to the atmosphere is proportional to SSTs and the surface wind speed (Gao et al., 2016; Gao, Zhai, et al., 2017). Using observational data from satellites for the Western North Pacific cyclones, Gao et al. (2016) show that the contribution of the latent heat flux in cyclone intensification is larger as compared to the sensible heat flux. This observation is similar to other cyclones across different basins (Jaimes et al., 2015; Lin et al., 2009; Shay & Uhlhorn, 2008; Uhlhorn & Shay, 2012). Various studies show that the intensification of cyclones is accompanied by an increase in the ocean-atmosphere latent heat flux (Bao et al., 2000; Li, 2004; Wu et al., 2005). Using idealized model simulations, Murthy & Boos, (2018) show that the ocean to atmosphere surface enthalpy fluxes is necessary for cyclone spin-up and its intensification. There is a two-way ocean-atmosphere interaction during cyclones (Emanuel, 1986). High SSTs favor an increase in the intensity of tropical cyclones through flux transfer from the ocean to the atmosphere (Emanuel, 1986). On the other hand, the passage of a cyclone induces cold ocean wakes, which in turn reduces the intensity of cyclones (Kaplan & DeMaria, 2003). This reduction in the intensity of cyclones is due to the decrease in the heat flux transfer from the ocean to the atmosphere owing to cold ocean wakes, as shown by observational studies (Cione & Uhlhorn, 2003; Lloyd & Vecchi, 2011) and modeling results (Bender & Ginis, 2000; Schade, 2000; Schade & Emanuel, 1999).

The north Indian Ocean, including the Arabian Sea and the Bay of Bengal, has two cyclone seasons in a year, April–June (pre-monsoon season) and October–December (post-monsoon season). It accounts for ~6% of global cyclone activity (Singh & Roxy, 2022). The ocean response to cyclones in the north Indian Ocean is significantly different during the two cyclone seasons. In the Bay of Bengal, on average, the cyclone-induced cooling in the pre-monsoon season is 2ºC-3°C (Krishna et al., 1993; Rao, 1987; Sengupta et al., 2008). However, in the post-monsoon season, the average cooling is 0.5ºC-1ºC (Sengupta et al., 2008). Similarly, cyclone-induced SST cooling in the Arabian Sea is more in the pre-monsoon season than in the post-monsoon season (Neetu et al., 2012). This varying ocean response to cyclones in the pre-monsoon and post-monsoon

seasons is mainly due to the different ocean characteristics in the two seasons (Neetu et al., 2012; Sengupta et al., 2008). In the Bay of Bengal, during the pre-monsoon season, larger cyclone-induced cooling is mainly because of weaker ocean stratification due to thin barrier layer which leads to higher ocean mixing and enhanced cooling during cyclone passage (Li et al., 2017). On the other hand, in the post-monsoon season, high fresh water influx into the basin enhances the ocean stratification with fresh water at the surface and saline water in the ocean sub-surface (Vinayachandran et al., 2002) which leads to the formation of a shallow mixed layer and thick barrier layer (Thadathil et al., 2007). The presence of a thick barrier layer inhibits the cyclone-induced mixing and restricts the upwelling of colder sub-surface water to the surface resulting in less cyclone-induced cooling as compared to the pre-monsoon season (Vissa et al., 2013). In the Arabian Sea, larger cyclone-induced cooling during the pre-monsoon season is due to higher cyclone wind power input (Neetu et al., 2012). On the other hand, during the post-monsoon season, the presence of ocean thermal stratification inhibits cyclone-induced cooling (Neetu et al., 2012; Subrahmanyam et al., 2005).

Previous studies have focused on the ocean-cyclone interaction in the north Indian Ocean with a focus on the ocean response to cyclones; however, these studies have not highlighted the influence of cyclones on the atmosphere. The transfer of heat flux from the ocean to the atmosphere is the major source of energy for cyclones. The condensation of water vapor in the updrafts of cyclones releases a large amount of latent heat, which is then transformed into kinetic and potential energy (Hack & Schubert, 1986; Nolan et al., 2007). The amount of latent heat released in a cyclone is directly proportional to the intensity of cyclones (Wu et al., 2021). Observations of cyclones in the North Atlantic Ocean show that the latent heat release in the eyewall of the cyclone plays an important role in their rapid intensification (Rogers et al., 2013, 2015). Similarly, for the Northwest Pacific Ocean cyclones, Yu & Yao, (2011) show that increased latent heating with height near the cyclone's inner core in the middle and upper troposphere provides a conducive condition for the intensification of cyclones. Anomalous warm temperatures at higher levels lead to higher pressure drop at the surface in cyclones as compared to the warming at the lower-level ones due to the amplification effects of the higher-level warming based on the hydrostatic balance (Chen & Zhang, 2013; Hirschberg & Fritsch, 1993). Using dropsonde data for nine cyclones from different basins, Durden (2013) reported that the height of the warm core in cyclones varied from 760-250 hPa and the intensity of cyclones is directly proportional to the strength and height of the warm core.

Similarly, theoretical studies suggested that the location of the release of the latent heat within a cyclone is crucial in determining the extent of the intensification of cyclones (Hack & Schubert, 1986; Schubert & Hack, 1982). Hu et al., (2019) show that in the Northwest Pacific Ocean, the latent heat released in the cyclones varies with their lifecycle. During the developing stage of cyclones, the latent heat is released mainly in the upper level of the atmosphere. On the other hand, during the mature stage of cyclones, latent heat is mainly released

in the lower level of the atmosphere (Hu et al., 2019). Observational data for the Northwest Pacific Ocean cyclones during the period 2000–2009 show that on average, the magnitude of the upper-level heating due to cyclones is about 2°C-2.5°C (Gao et al., 2019). A similar analysis using the Atmospheric Infrared Sounder (AIRS) temperature profiles shows that the magnitude of upper-level heating is found to be in the range of 10°C-12°C for category 4 and category 5 cyclones (Gao et al., 2017). A modelling study for Cyclone Wilma shows the reduction in the SSTs by 1°C, significantly reduces the upper-level warm core within the cyclone (Chen & Zhang, 2013). This is because cooler SSTs reduce the convective instability and the convective available potential energy (Chen & Zhang, 2013).

The latent heat is generally released in the middle to upper troposphere (Adler & Rodgers, 1977; Kuo, 1965) and directly depends on the amount of condensate in the clouds (Nolan et al., 2019; Yanai et al., 1973). Observational analysis for super Cyclone Paka shows that the latent heat release processes vary with height (Rodgers et al., 2000). In the lower level, convective processes are the major source of latent heat release and in the middle to upper levels, cloud ice microphysical processes play a dominant role in the latent heat release (E. Rodgers et al., 2000). Modelling analysis for Cyclone Andrew (1992) shows that warm rain processes in cyclone clouds play a major role in the total latent heat release compared to the mixed-phase processes (Zhang et al., 2002). Using the observational analysis for convective clouds, Tong et al. (1998) show that the smaller contribution of freezing and melting to the total heating in a convective cloud is due to the smaller value of latent heat of fusion. For cyclones, observation suggests that the distribution of type of precipitate in the cloud, especially in the eyewall region, is significantly different from a convective thunderstorm cloud (Black et al., 2003). They show that in a cyclone eyewall supercooled liquid water exists even in the upper levels of the atmosphere (Black et al., 2003). Contrary to the mid to upper-level heating in cyclones, evaporative cooling is observed in the lower troposphere of the cyclone (Rodgers et al., 1998).

A large amount of latent heat release in cyclones amplifies the clouds buoyancy and enhances the updrafts ascending motion within the cloud mainly in the mid to upper level of the atmosphere (Jorgensen, 1984; Lord et al., 1984). Black et al. (1994) documented very strong updrafts of magnitude 24 m s^{-1} at the height of 5 km within the eyewall of Hurricane Emily (1987). Similarly, using the aircraft data, Aberson et al. (2017) reported updrafts of magnitude 31 m s^{-1} in Hurricane Felix (2007) at 700 hPa. Based on aircraft and doppler radar observations, Black et al. (1994) show that for Hurricane Emily (1987), the maximum velocity of the updrafts in the eyewall is near the melting level. These updrafts play a crucial role in determining the intensity of cyclones and the system's energy balance.

While several studies have investigated the upper-atmospheric response in the northwest Pacific and North Atlantic oceans, a comprehensive understanding of the atmospheric response to cyclones is lacking in the north Indian. Earlier

studies have shown that the ocean-cyclone interaction in the Arabian Sea and the Bay of Bengal differs in the two cyclone seasons (Neetu et al., 2012; Sengupta et al., 2008). However, how the different ocean-cyclone interactions in the two seasons can influence the atmospheric response to cyclones is unclear. Therefore, the main objective of this study is to understand the atmospheric response to cyclones in the north Indian Ocean during the pre-monsoon and post-monsoon seasons.

2. Data and Methodology

2.1. Data

To understand the atmospheric response to cyclones in the north Indian Ocean, we have analyzed the cyclones during the period 1982–2019. The cyclone data for this period is obtained from Joint Typhoon Warning Center (JTWC) as archived in the International Best Track Archive for Climate Stewardship (IBTrACS) cyclone dataset (Knapp et al., 2010). In the north Indian Ocean, we have analyzed the atmospheric response to cyclones separately for the Arabian Sea and the Bay of Bengal in the pre-monsoon and the post-monsoon seasons. To understand the role of SSTs in the atmospheric response to cyclones, the daily SST data for the above-mentioned period, at a spatial resolution of 0.25° × 0.25° is obtained from the Optimum Interpolation Sea Surface Temperature (OISST) dataset provided by the National Oceanic and Atmospheric Administration (NOAA) (Reynolds et al., 2007). Latent heat flux data at a spatial resolution of 0.25° × 0.25° is obtained from the European Center for Medium Range Weather Forecasts (ECMWF) fifth-generation global atmospheric reanalysis (ERA5) dataset (Hersbach et al., 2020). A recent study by Pokhrel et al. (2020) show that in the north Indian Ocean, the flux estimates by ERA5 are the best among the various available reanalysis datasets. The convention of the latent heat flux used in this study is — positive means the heat flux is transferred from the ocean to the atmosphere. To see the atmospheric response to cyclones in the two cyclone seasons, various other atmospheric variables such as atmospheric temperature, specific humidity, relative humidity, vertical velocity at multiple atmospheric levels, and outgoing longwave radiation (OLR) are also obtained from ERA5 at a spatial resolution of 0.25° × 0.25°. For the analysis of various ocean-atmosphere parameters, daily anomalies are obtained by using the daily climatology for the period 1982–2019. The student's two-tailed t test is applied to analyze the statistical significance of the results.

2.2. Methodology

We have analyzed the evolution of the composite of various ocean and atmospheric parameters anomalies averaged over 1° × 1° grid area that is roughly 100 km radius around each cyclone center position. The evolution of ocean-atmosphere parameters is studied before, during, and after the cyclone passage. We considered cyclogenesis day as the day when the system has attained a maximum sustained wind speed of 20 knots. We have excluded the days when the cyclone has made landfall and its center is over the land. This is because

land-cyclone interaction is different as compared to the ocean-cyclone interaction due to the land induced friction and absence of moisture supply from the ocean. We calculated the number of cyclone days from its genesis till landfall or open ocean dissipation for every cyclone. Those cyclones that have crossed from the Bay of Bengal into the Arabian Sea are considered Bay of Bengal cyclones until landfall over India or Sri Lanka east coast. After these cyclones reemerge into the Arabian Sea, they are considered as Arabian Sea cyclones. Using this methodology, the total number of cyclone days in the Arabian Sea during the pre-monsoon season is 154 and the post-monsoon season is 270, for the period 1982–2019. Similarly, the total number of cyclone days in the Bay of Bengal during the pre-monsoon season is 182 and the post-monsoon season is 429. Generally, the ocean and atmosphere start getting affected by a cyclone from one to two days before the cyclone center passes that location. We have analyzed the evolution of the composite of ocean-atmosphere anomalies starting from seven days before the passage of cyclones over each location on the track, as it will help us to understand the prevailing pre-cyclone ocean-atmosphere conditions. Day 0 is the day of passage of cyclones, day -7 to day -1 are seven to one days before the passage of cyclones, and day +1 to day +16 are one to sixteen days after the passage of cyclones.

Previous studies have shown that latent heat flux depends on the SST, surface wind speed, and the difference in the specific humidity between the ocean and the lower atmosphere (Gao et al., 2016; Jaimes et al., 2015). To estimate the dominant factor contributing to the latent heat flux, we have used the bulk aerodynamic formula for the latent heat flux which is given by equation 1 (Fairall et al., 2003).

$\mathrm{LHF} = \mathrm{LC_E U(q_s\text{-}q_a)}$ Equation 1

Where, is the density of air having a value of 1.17 x 10^{-6} g m^{-3}, and L is the latent heat of evaporation of water having value of 2360 J g^{-1}. C_E is the bulk transfer coefficient for latent heat flux, a unitless quantity, and its value estimated for the Indian Ocean is 1250 (M. Roxy et al., 2013). U and q_a are the wind speed (m s^{-1}) and specific humidity (g kg^{-1}) respectively at a height of 10 m above the surface and q_s is the saturation specific humidity at sea surface temperature. The difference q_s-q_a is called moisture disequilibrium (Jaimes et al., 2021), a key factor determining the intensity of the fluxes. Recent research shows that among various reanalysis datasets, cyclones in the north Indian Ocean are best represented in the ERA5 reanalysis dataset (Malakar et al., 2020). Hence, the winds at 10 m along the track of the cyclone around 1°×1° cyclone center are obtained from the ERA5 reanalysis dataset.

To estimate how close the air is to saturation, we computed the dew point depression. It is derived by taking the difference between the actual atmospheric temperature and the dew point temperature, as shown in equation 2 (Lawrence, 2005).

$T_{\mathrm{dd}} = T - T_d$ Equation 2

Where T_{dd} is the dew point depression, T is the atmospheric temperature (K) and T_d is the dew point temperature (K). As the dew point depression increases, the air becomes drier and relative humidity decreases. To compute the dew point depression, first we calculated the dew point temperature (T_d) using the estimates of vapor pressure and saturation vapor pressure and Clausius-Clapeyron relationship, as shown in Equations 3, 4, and 5.

$RH = 100\% \times (\frac{E}{Es})$ Equation 3

According to an approximation of Clausius-Clapeyron equation:

$e = e_0 \times \exp\left[\left(\frac{L}{R_v}\right) \times \left\{\left(\frac{1}{T_0}\right) - \left(\frac{1}{T_d}\right)\right\}\right]$ Equation 4

$e_s = e_0 \times \exp\left[\left(\frac{L}{R_v}\right) \times \left\{\left(\frac{1}{T_0}\right) - \left(\frac{1}{T}\right)\right\}\right]$ Equation 5

Where RH is the relative humidity (%), e is the vapor pressure and e_0 is the saturation vapor pressure at a known temperature (T_0), $e_0 = 0.611$ kPa, (L/R_v) = 5423 K (over the flat surface of water), $T_0 = 273.15$ K, T_d is the dew point temperature (K) and T is the actual atmospheric temperature (K).

1. **Results**

   (a) **Ocean-cyclone coupled interaction**

      i. Contrasting SST response to cyclones in the two seasons

To understand the ocean-cyclone interaction, we analyzed the evolution of the SSTs from day -7 to day +16 for the cyclones in the Arabian Sea and the Bay of Bengal during the two cyclone seasons (Figure 1a,b). It can be seen from Figure 1a that in the Arabian Sea, during the pre-monsoon season, the pre-cyclone SSTs (average SSTs from day -7 to day -3) are ~30.0°C. Similarly, in the Bay of Bengal, during the pre-monsoon season, the pre-cyclone SSTs are 29.9°C (Figure 1b). On the contrary, in the post-monsoon season, in both the basins, the pre-cyclone SSTs are significantly (statistically significant at 99.99% confidence levels) lower than the pre-monsoon season. The pre-cyclone SSTs in the Arabian Sea and Bay of Bengal during the post-monsoon season are 28.2°C and 28.5°C respectively (Figure 1a,b). This is in line with the previous study by (Singh & Roxy, 2022), which shows that in the north Indian Ocean, the pre-cyclone SSTs in the pre-monsoon season are warmer than the post-monsoon season.

Similar to the actual SSTs, an analysis of the SST anomalies shows that during the pre-monsoon season, in both basins, anomalous positive SST anomalies persist before the passage of the cyclone (Figure 1c and d). From day -2 (2 days before the passage of the cyclone), the SST anomalies start decreasing rapidly. This SST decrease is mainly due to the interaction of the outer periphery of the cyclone with the ocean, leading to the mixing and upwelling of cooler subsurface water to the surface. By day 0, the SST anomalies decreases by 0.49°C in the Arabian Sea and by 0.24°C in the Bay of Bengal, as compared to the SST anomalies before the passage of the cyclone (average SST anomalies from day

-7 to day -3). After the passage of the cyclone, the SSTs continue to decrease, and the average post-cyclone (average SST anomalies from day +3 to day +7) SST anomalies are 1.18°C and 1.09°C cooler than the pre-cyclone SSTs in the Arabian Sea and the Bay of Bengal respectively (Figure 1c,d). The continued decrease in SST even after the passage of cyclone is due to the upwelling, which continues for a few days after cyclone passage. Similar continued cooling of SSTs for a few days after the passage of cyclones is observed in other basins globally (S. Wang & Toumi, 2021).

On the contrary, the SST anomalies before the passage of cyclone are significantly lower (statistically significant at 99% confidence level) during the post-monsoon season in both the Arabian Sea and the Bay of Bengal. Also, it can be seen that in the Bay of Bengal, no positive SST anomalies are seen before cyclone which is in contrast to the pre-monsoon season. The average post-cyclone SSTs anomalies are 0.63°C and 0.28°C cooler than the pre-cyclone SSTs in the Arabian Sea and the Bay of Bengal respectively (Figure 1c,d). This shows that in the Arabian Sea and the Bay of Bengal, the cyclone-induced SST cooling is 46.6% and 74.3% less than in the pre-monsoon season. The difference in the cooling between the two seasons is statistically significant at 99% confidence level. This difference in the cooling during the two seasons is in agreement with the previous findings (Neetu et al., 2012; Sengupta et al., 2008). The main reason for the contrasting ocean response in the two cyclone seasons is the presence of a thick barrier layer in the Bay of Bengal during the post-monsoon season. This inhibits cyclone-induced mixing and upwelling, resulting in less cooling than the pre-monsoon season (Vissa et al., 2013). Whereas, in the Arabian Sea, ocean thermal stratification inhibits cyclone-induced cooling (Neetu et al., 2012; Subrahmanyam et al., 2005b).

1. Contrasting latent heat flux exchange during cyclones in the two seasons

Studies for different ocean basins have shown that the SSTs fuel the cyclones by providing heat flux from the ocean to the atmosphere. Among the heat fluxes, the latent heat flux plays a dominant role in energizing the cyclone compared to the sensible heat flux (Jaimes et al., 2015; Lin et al., 2009). Therefore, our analysis is focused on understanding the characteristics and evolution of the latent heat flux exchange from the ocean to the atmosphere in the two cyclone seasons. We have analyzed the evolution of the latent heat flux and the latent heat flux anomaly along the track of cyclones averaged over a 1°×1° grid area around the cyclone's center from day -7 till day +16. However, only the evolution of latent heat flux anomaly is presented here in figures 2 a and b. Our analysis shows that during the pre-monsoon season, in the Arabian Sea, the average latent heat flux exchange from the ocean to the atmosphere on the day of cyclone (i.e. day 0) is 202.6 W m^{-2} which is 88.7 W m^{-2} more than normal (Figure 2a). On the other hand, in the Bay of Bengal, the average latent heat flux exchange from the ocean to the atmosphere on the day of cyclone is 196.6 W m^{-2} which is 96.4 W m^{-2} more than normal (Figure 2b). The magnitude of latent heat flux transfer during the pre-monsoon season is similar to that

reported during the cyclones in the Northwest Pacific Ocean (Gao et al., 2019).

On the contrary, the average latent heat flux during the post-monsoon cyclones on day 0 for the Arabian Sea is 148.9 W m^{-2} which is 52.9 W m^{-2} more than normal, and for the Bay of Bengal is 159.7 W m^{-2} which is 50.3 W m^{-2} more than normal (Figure 2a and b). These results show that there is a sharp contrast in the air-sea flux exchange in the two cyclone seasons. Significantly (statistically significant at 99% confidence level) higher latent heat flux is transferred from the ocean to the atmosphere in the pre-monsoon season as compared to the post-monsoon season.

1. Mechanism driving the contrasting latent heat exchange in the two seasons

To see the mechanism leading to the higher latent heat flux exchange from the ocean to the atmosphere during the pre-monsoon season, we utilized the latent heat flux bulk formula, as shown earlier in equation 1. Studies have shown that latent heat flux from the ocean to the atmosphere is directly proportional to the SSTs (Gao et al., 2016; Gao et al., 2017). From equation 1, it can be seen that two different mechanisms control the latent heat exchange during cyclones. First is the mechanically driven heat uptake, which is an increase in evaporation from the sea surface with the increase in the near-surface wind speed. Second is the thermodynamically driven heat uptake caused by the moisture differences between the sea surface and near the sea surface. For the cyclones in the North Atlantic Ocean, it is observed that in the regions of high wind speed of cyclone, even slight SST changes significantly alter the moisture disequilibrium, which in turn changes the latent heat flux exchange from the ocean to the atmosphere (Cione & Uhlhorn, 2003). This moisture disequilibrium is mainly determined by the saturation specific humidity at the ocean surface and is a function of SSTs rather than the near-surface atmospheric specific humidity (Jaimes et al., 2015). Analyzing the North Atlantic Ocean cyclones, Cione & Uhlhorn (2003) show that an increase in SSTs by 1°C increases the flux exchange from the ocean to the atmosphere by 40%. An increase in the moisture disequilibrium increases the latent heat flux from the ocean to the atmosphere (Cione et al., 2013). Based on the bulk formula of the latent heat flux as shown in equation 1, we have estimated the moisture disequilibrium between the ocean surface and the near-surface for the cyclone day (i.e., at day 0) at each cyclone location averaged over 1°×1° region around the center of the cyclone. The results are presented in Table S1. It can be seen from Table S1 that during the pre-monsoon season, the mean moisture disequilibrium in the Arabian Sea and the Bay of Bengal is 6.33 g kg^{-1} and 6.92 g kg^{-1} respectively. This moisture disequilibrium during cyclones in both basins is higher than in the Northwest Pacific Ocean cyclones (Gao et al., 2016). This indicates the potential of higher latent heat flux transfer during cyclones in the north Indian Ocean as compared to the Northwest Pacific Ocean basin. On the other hand, during the post-monsoon season, the mean moisture disequilibrium in the Arabian Sea and the Bay of Bengal is 5.40 g kg^{-1} and 5.86 g kg^{-1} respectively. This shows that in both the basins, the moisture disequilibrium is higher during the pre-

monsoon season than the post-monsoon season. During the pre-monsoon season, on the day of the cyclone, the correlation between the latent heat flux and the moisture disequilibrium in the Arabian Sea and the Bay of Bengal is 0.30 and 0.23 respectively which is statistically significant at 99% confidence level (Figure 3a and c). Whereas, during the post-monsoon season, the correlation between the latent heat flux and moisture disequilibrium in the Arabian Sea and the Bay of Bengal is (r=0.13) (statistically significant at 95% confidence level) and (r=0.32) (statistically significant at 99% confidence level) respectively (Figure 3b and d).

Gao et al. (2016) show that for the cyclones in the Northwest Pacific Ocean, higher moisture disequilibrium between the ocean and atmosphere is due to higher SSTs leading to increased latent heat flux transfer fueling the intensification of cyclones. In line with earlier studies, from the correlation analysis in figure 4, we see a significant positive correlation between the moisture disequilibrium and the SSTs in both the basins and seasons. The higher moisture disequilibrium during the cyclones in the pre-monsoon season in both the basins is attributed to the higher SSTs in this season compared to cyclones in the post-monsoon season (Figure 1a, b).

The latent heat flux also depends on the near-surface wind speed i.e., winds at 10 m, as shown by equation 1. We find that the average observed wind speed at 10 m on the day of cyclone (i.e., day 0) is 9.27 m s^{-1} during the pre-monsoon season in the Arabian Sea, whereas in the Bay of Bengal, it is 8.23 m s^{-1} (Table S1). On the other hand, the average observed wind speed at 10 m on the day of cyclone is 7.99 m s^{-1} during the post-monsoon season in the Arabian Sea, whereas in the Bay of Bengal, it is 7.90 m s^{-1}. Since we are averaging over a 1°×1° region around the cyclone center, the cyclone's wind speed will be less than the maximum wind speed as per JTWC records. For comparison with the observations, we estimated the average maximum winds of the cyclone as archived by JTWC. The average maximum wind speed of cyclones during the pre-monsoon season in the Arabian Sea is 35.9 m s^{-1} and in the Bay of Bengal is 37 m s^{-1}. Whereas, during the post-monsoon season, the cyclone's average maximum wind speed is 30.8 m s^{-1} and 31.2 m s^{-1} in the Arabian Sea and the Bay of Bengal, respectively. Thus, it can be seen from the ERA5 and from the JTWC observations that, on average, the wind speed at 10 m during cyclones is higher during the pre-monsoon season than during the post-monsoon season. The difference in the wind speeds between the two seasons for both the basins on the day of cyclones is statistically significant at 99% confidence level. This is in line with the previous study by Li et al. (2013) which show that on average stronger cyclones form in the Bay of Bengal during the pre-monsoon season as compared to the post-monsoon season.

From Figure 5, it can be seen that with the increase in the wind speed of cyclones, there is a corresponding increase in the latent heat flux in both the basins and seasons. During the pre-monsoon season, the correlation between the latent heat flux and the wind speed at 10 m in the Arabian Sea and the Bay

of Bengal is (r=0.85) and (r=0.90) respectively which is statistically significant at 99% confidence level. During the post-monsoon season, this correlation for the Arabian Sea and the Bay of Bengal is (r=0.82) and (r=0.87), respectively, which is also statistically significant at 99% confidence level (Figure 5b and d). Hence, it can be inferred that the latent heat flux exchange in both basins strongly depends on the cyclone's wind speed.

The analysis above shows that in the north Indian Ocean, the latent heat flux exchange is directly proportional to the near-surface wind speed of the cyclone and the moisture disequilibrium. Also, the moisture disequilibrium increases with an increase in the SSTs. This is in agreement with a recent study on cyclones in the North Atlantic Ocean (Jaimes et al., 2021). Further, in the Arabian Sea and the Bay of Bengal, the SSTs, cyclone wind speed, and moisture disequilibrium are higher during the pre-monsoon season than the post-monsoon season. As a result, there is a higher latent heat flux exchange from the ocean to the atmosphere in the former than in the latter season.

1. **Atmospheric response to cyclones in the north Indian Ocean**

   (a) Changes in the atmospheric temperature in response to cyclones

In the earlier sections, we have seen that during cyclones in the Arabian Sea and the Bay of Bengal, there are significantly high SSTs and latent heat flux exchange from the ocean to the atmosphere in the pre-monsoon season, as compared to the post-monsoon season. Such a contrasting ocean-cyclone interaction in the two seasons can have significantly different atmospheric response too. To understand the atmospheric response to cyclones in the two basins and the two cyclone seasons, we first analyzed the atmospheric temperature anomaly at different atmospheric levels for cyclone day at each cyclone location.

During the pre-monsoon season, in the Arabian Sea, on the day of the cyclone, large anomalous warming is observed at the upper levels (200-400 hPa), with maximum warming at 300 hPa (Figure 6a). The temperature anomalies at 300 hPa and 400 hPa are 3.74°C and 3.41°C respectively. Similarly, in the Bay of Bengal, on the day of the cyclone, anomalous large upper-level atmospheric warming is observed with temperature anomalies at 300 hPa and 400 hPa are 3.32°C and 3.11°C respectively (Figure 6b). In both the basins, anomalous upper-level warming starts decreasing from day +2, that is, two days after the passage of cyclone (figure not shown). This shows that anomalous upper-level warming is tightly coupled with the cyclone. The upper-level cyclone-induced warming observed in the Arabian Sea and the Bay of Bengal is similar to the cyclone-induced upper-level warming observed in the North Atlantic Ocean and Northwest Pacific Ocean basin (Gao et al., 2019; Zawislak & Zipser, 2014). Further, the anomalous warm temperature anomalies at 300 hPa are consistent with the theoretical estimate of Emanuel (1986).

During the post-monsoon season, the cyclones in the Arabian Sea and the Bay of Bengal induce anomalous maximum warming at 300 hPa, similar to the pre-monsoon season. However, in this season, the magnitude of the cyclone-induced

upper-level warming is significantly less (statistically significant at 99% confidence level) than in the pre-monsoon season (Figure 6a, b). The mean cyclone-induced anomalous warming at 300 hPa in the Arabian Sea and the Bay of Bengal is 1.27°C and 1.15°C respectively, which is just one-third compared to the pre-monsoon season. In the next section, we will discuss the mechanism driving this contrasting cyclone-induced upper-level warming in the two cyclone seasons.

Contrary to the anomalous upper-level warming on the cyclone day in the north Indian Ocean, there is an anomalous cooling at the lower levels from 850 hPa to 1000 hPa (Figure 6a and b). The low-level cooling is more intense during the pre-monsoon season than the post-monsoon season. During the pre-monsoon season, the maximum low-level cooling is observed at 850 hPa. Anomalous intense cooling is observed in the Arabian Sea compared to the Bay of Bengal and the difference in cooling between the basins is 1.5°C at 850 hPa (Figure 6a, b). Similar to the upper levels, there is also a contrast in the low level-cooling between the pre-monsoon and the post-monsoon seasons. During the post-monsoon season, the anomalous low-level cooling in both basins is significantly less (statistically significant at 99% confidence level) than in the pre-monsoon season. In the Arabian Sea, the maximum anomalous cooling of magnitude -0.29°C is observed at 850 hPa. Whereas, in the Bay of Bengal, maximum anomalous cooling of magnitude -0.43°C is observed at 1000 hPa. In general, the center of the cyclone (that is, the eye region) has anomalous warmer temperatures due to the subsidence occurring in the cyclone center (Willoughby, 1998). Since we are averaging over a wider area that is 1°×1° around the center of the cyclone, it includes both the eye of the cyclone and the eyewall region, which is the precipitation region. Based on the aircraft observation of the cyclone in the Atlantic, Houze et al. (2009) show that the precipitation from the cyclone clouds leads to evaporative cooling beneath the base of clouds resulting in anomalous low-level cooling. In the later section, we will analyze the role of evaporative cooling in anomalous low-level cooling.

1. Mechanism driving the contrasting cyclone induced upper-level warming in the two cyclone seasons

In the previous section, we see that, similar to the ocean response, the atmospheric response to cyclones in the two cyclone seasons is also significantly different. Earlier, we have seen that during cyclones, the latent heat flux transfer from the ocean to the atmosphere is significantly larger during the pre-monsoon season compared to the post-monsoon season. The enhanced latent heat flux exchange from the ocean to the atmosphere during the pre-monsoon season increases the vertically averaged (averaged from 1000-500 hPa) specific humidity (henceforth will be called as averaged lower to mid-troposphere specific humidity) as shown in Figures S1a and b. During the pre-monsoon season, the averaged lower to mid-troposphere specific humidity on the day of cyclone in the Arabian Sea is 12.26 g kg^{-1}, which is 4.77 g kg^{-1} above normal. Similarly, in the Bay of Bengal, it is 12.29 g kg^{-1}, which is 3.36 g kg^{-1} above normal. The

anomalous higher specific humidity at low to middle levels is similar to the observation for cyclones in the Northwest Pacific Ocean (Gao et al., 2019). Gao et al. (2019) show that in the Northwest Pacific Ocean, during cyclones, the anomalous moisture in the atmosphere is injected by the anomalous high latent heat flux exchange from the ocean to the atmosphere. Similar to the Northwest Pacific Ocean, we observe that during the pre-monsoon season, there is a statistically significant correlation between the anomalous latent heat and the specific humidity at 850 hPa. The correlation is (r = 0.31) in the Arabian Sea and (r = 0.52) in the Bay of Bengal. Since the maximum anomalous specific humidity is observed at 850 hPa in both basins, the correlation with the latent heat flux is shown only for this level. The positive correlation indicates that with the increase in the latent heat flux exchange from the ocean to the atmosphere, there is a corresponding increase in moisture in the lower atmosphere. This anomalous moisture is then transported upwards by the cyclone secondary circulation leading to an increase in moisture in the entire lower to middle atmospheric column (Gao et al., 2019).

On the contrary, during the post-monsoon season, the lower to mid-troposphere specific humidity is less as compared to the pre-monsoon season (Figure S1a-d). In the Arabian Sea, it is 10.85 g kg^{-1} which is 11.5% less than the pre-monsoon season. Similarly, in the Bay of Bengal, it is 11.24 g kg^{-1} which is 8.5% less than the pre-monsoon season. The difference in the average lower to mid-troposphere specific humidity between the pre-monsoon and post-monsoon seasons is statistically significant at 99% confidence level. Anomalous lower specific humidity on the day of cyclone during the post-monsoon season as compared to the pre-monsoon season is attributed to the anomalous lower latent heat flux exchange in the former season than in the latter season (Figure 2a and b).

We further analyzed the average OLR on the day of the cyclone (day 0), averaged over a 1°×1° area around the cyclone center at each cyclone location. This analysis is carried out to study the convection in the pre-monsoon and post-monsoon seasons in the two basins. OLR is used as a proxy to study tropical convection, anomalous high OLR denotes suppressed convection and anomalous low OLR denotes enhanced convection (see for example (Lau & Chan, 1986). We found that during the pre-monsoon season, the mean OLR on the day of cyclone in the Arabian Sea is 164.8 W m^{-2} which is 108.8 W m^{-2} below normal and in the Bay of Bengal, it is 140.6 W m^{-2} which is 107.5 W m^{-2} below normal. Whereas, during the post-monsoon, the mean OLR on the day of cyclone in the Arabian Sea is 186.4 W m^{-2} which is 72.1 W m^{-2} below normal and in the Bay of Bengal, it is 162.9 W m^{-2} which is 65.9 W m^{-2} below normal (Table 1). The difference in the OLR between the two seasons for both basins is statistically significant at 99% confidence level. This shows that in both basins, the convection on the day of the cyclone during the pre-monsoon season is more intense than the post-monsoon season.

In the earlier section, we have seen that on the day of cyclone, the latent heat

flux and mid to lower troposphere specific humidity are higher during the pre-monsoon season as compared to the post-monsoon season. Young et al. (1992) show that convection increases with an increase in the latent heat flux. Similar to this, from the scatter plot shown in Figure S2, we find that with the increase in the latent heat flux there is a corresponding decrease in OLR in both the basins. This indicates an increase in the convection with an increase in the latent heat flux. During the pre-monsoon season, the correlation between the latent heat flux anomalies and OLR anomalies is (r = -0.35) in the Arabian Sea and (r = -0.50) in the Bay of Bengal (Table 1). Whereas, during the post-monsoon season, this correlation is (r = -0.41) in the Arabian Sea (Table 1). However, in the Bay of Bengal, the correlation is weak (r = -0.24), which indicates that the dependence of convection on the latent heat flux is weak as compared to the Arabian Sea. The varying dependence of convection on the latent heat flux in the two basins is out of the scope of this study. Despite this contrast, the correlation between the latent heat flux anomalies and OLR anomalies in both the basins and seasons is statistically significant at 99% confidence level. This shows that atmospheric convection is directly proportional to the latent heat flux exchange from the ocean to the atmosphere. Since the convection (OLR) is directly dependent on the latent flux exchange, we see that the convection in the cyclone is intense in the pre-monsoon season than the post-monsoon season due to higher latent heat flux exchange during the former season as compared to the latter season (Table 1).

On the day of cyclone during the pre-monsoon season, the intense convection is simultaneously accompanied by intense updrafts (denoted by the negative vertical velocity anomalies in Figures 6c and d) in both the basins. Strong convergence in the eyewall of a cyclone at low levels and strong outflow at the upper levels must be balanced by strong upward vertical motion between the lower and upper levels (Houze, 2010). In the Arabian Sea, the peak in the updraft velocity is observed at 600 hPa, whereas in the Bay of Bengal, the peak is observed at 500 hPa (Figure 6c and d). The magnitude of the peak updraft anomalous velocity is -0.77 Pa s^{-1} in the Arabian Sea and -0.57 Pa s^{-1} in the Bay of Bengal (Figure 6c and d). These mid-level maxima in the updraft velocity for the north Indian Ocean cyclones are similar to the aircraft observations for the cyclones in the North Atlantic Ocean (Black et al., 1994; Frank, 1977; Jorgensen, 1984). The higher updraft velocity in the mid-levels as compared to the lower levels is because the largest virtual temperature anomalies exist above the freezing level. Also, the latent heat released by freezing water droplets and the growth of ice crystals enhances the cloud buoyancy, thus increasing the updraft velocity in the mid-levels (Braun, 2002; Eastin et al., 2005; Houze, 2010).

Contrary to the pre-monsoon season, the updrafts are less intense during the post-monsoon season in both the Arabian Sea and the Bay of Bengal (Figure 6c and d). In this season, the peak updraft anomalous velocity in the Arabian Sea is -0.42 Pa s^{-1} and in the Bay of Bengal is -0.43 Pa s^{-1}. In both the basins, the difference in the intensity of peak updrafts between the two seasons is sta-

tistically significant at 99% confidence level. We computed the average updraft velocity at the pressure level where maximum updrafts are observed in both the basins, that is, 500-600 hPa (Table 1). The correlation between the average mid-level updraft and the OLR is moderate but is significantly positive (statistically significant at 99% confidence level) for both the basins and the seasons (Table 1). However, a moderate positive correlation indicates that the intensity of updrafts is dependent not only on the strength of convection in the cyclone but also on other factors. Since, on the day of cyclone, the pre-monsoon season cyclones have stronger convection as compared to the post-monsoon season cyclones; therefore, the updrafts in the cyclone in the former season are stronger as compared to the later season. A significant forcing that governs the updraft intensity in a cumulonimbus cloud is the buoyancy across the updraft width, which is largely determined by the virtual temperature anomalies, entrainment rate, and water loading in the cloud (Houze, 2010; Lucas et al., 1994). The role of these factors in governing the updraft variations during the cyclone between the pre-monsoon and the post-monsoon season is out of the scope of this study. We are averaging over $1^\circ \times 1^\circ$ area around the cyclone center, so the downward vertical velocity in the eye (center) of the cyclone as noted by Schubert et al., (2007) cannot be distinguished in our study.

The intense convection during cyclones in the pre-monsoon season leads to enhanced latent heat release in the mid to upper atmosphere, as seen from the air temperature anomalies. The generation of latent heat release above freezing level is due to the ice microphysical processes (Rodgers et al., 1998). Our results are in agreement with earlier studies for cyclones of other basins that the maxima in the latent heating are generally at mid to upper levels (Hack & Schubert, 1986; Nolan et al., 2007; Vigh & Schubert, 2009). Nolan et al. (2019), using numerical simulation of cyclones in the North Atlantic Ocean, show that the maxima of the total condensate in clouds of cyclone peaks at upper-levels 8-10 km, leading to maximum heating at these upper levels. As discussed earlier, the maximum anomalous warming on the cyclone day is observed at the upper level (300 hPa), similar to the findings for other basins. We have computed a correlation between the OLR and upper-level (300 hPa) temperature anomalies (Table 1). It can be seen from Table 1 that there is a statistically significant correlation between the OLR anomalies and the upper-level temperature anomalies in both the basins and seasons.

From the scatter plot shown in Figure S3, it is seen that with the increase in the latent heat flux anomalies, there is an enhancement of the anomalous upper-level warming. During the pre-monsoon season, the latent heat flux and upper-level temperature anomalies show a significant positive correlation ($r = 0.57$) in the Arabian Sea and ($r = 0.56$) in the Bay of Bengal. A similar correlation is seen during the post-monsoon season also. With the increase in the latent heat flux and convection, there is an increase in the moisture transport from the ocean to the atmosphere by the stronger updrafts and a large amount of latent heat of condensation is released into the upper atmosphere leading to anomalous warming. Earlier, we have seen that on the day of cyclone, the latent heat flux

transfer from the ocean to the atmosphere and the convection is stronger during the pre-monsoon season than the post-monsoon season. This results in enhanced latent heat of condensation release in cyclones during the pre-monsoon season compared to the post-monsoon season, leading to an enhancement of upper-level anomalous warming during the former season compared to the latter season (Figure 6a, b).

1. Mechanism driving the contrasting low-level cooling during cyclones in the two seasons

Section 3.2.1 shows that on the day of cyclone, there is a contrasting response of the atmospheric temperature between the upper and lower levels. Anomalous warming is observed in the upper levels and anomalous cooling in the lower levels, with a more pronounced signature in the pre-monsoon season than in the post-monsoon season (Figure 6a, b). From the principles of thermodynamics, it is well known that the rain falling through a drier atmosphere (low relative humidity) tends to evaporate more as compared to the rain falling through a humid atmosphere (high relative humidity) (Houze, 2010). A high rate of evaporation enhances evaporative cooling (Takemi, 1999). The dew point depression can be used as an index to measure the dryness in the atmosphere and is computed using equation 2. It shows the magnitude of temperature decrease that must occur to achieve 100% relative humidity (condensation). A higher dew point depression means that the difference between that actual temperature and the dew point temperature is large, indicating less relative humidity and dry atmosphere (Wang et al., 2019). Hence, to understand the possible factor governing low-level cooling, we investigate the low-level relative humidity and the dew point depression before cyclone.

Table S2 shows that before the cyclone (averaged from day -7 to day -3) the average relative humidity at 850 hPa is 47.51% in the Arabian Sea and 62.17% in the Bay of Bengal. This difference in the relative humidity at 850 hPa between the two basins is statistically significant at 99% confidence level. Also, from Table S2, we see that among the lower levels the maximum dew point depression is observed at 850 hPa in both the basins and seasons. During the pre-monsoon season, the dew point depression at 850 hPa before the cyclone (averaged from day -7 to day -3) in the Arabian Sea and the Bay of Bengal is 11.52 K and 7.38 K respectively. The correlation between the lower atmosphere (850 hPa) temperature anomalies and the averaged dew point depression (averaged from day -7 to day -3) at 850 hPa is (r = -0.38) in the Arabian Sea and (r = -0.33) in the Bay of Bengal. This correlation is moderate but is statistically significant at 99% confidence level. This negative correlation indicates that with an increase in the dew point depression (increase in the dryness of atmosphere) the lower atmosphere evaporative cooling increases leading to negative temperature anomalies. However, a moderate correlation also indicates that atmospheric humidity is not the only driver regulating the low-level evaporative cooling, and there might be other factors involved too (discussed later in the discussion section). Since the maximum dew point depression in the lower levels is observed at 850 hPa (Ta-

ble S2), the evaporative cooling is also maximum at this level (Figure 6a and b). In both the basins, the dew point depression gradually decreases from day -7 to day 0 (Figure 7) and a corresponding increase in the relative humidity is observed (figure not shown). This is due to the cyclone effect, the moisture in the atmosphere increases, leading to a decline in the dew point depression and an increase in the relative humidity. On the day of cyclone (day 0), the dew point depression in both the basins reduces to less than 2 K. From Tables S2, it can be seen that during the pre-monsoon season, dew point depression is higher in the Arabian Sea than in the Bay of Bengal, leading to lower relative humidity in the former than the latter basin. This results in enhanced evaporative cooling on the day of cyclone in the Arabian Sea than in the Bay of Bengal.

During the post-monsoon season, in both the basins, the relative humidity at 850 hPa before the cyclone (averaged from day -7 to day -3, table 3) is significantly higher than in the pre-monsoon season (Table S2), which is in agreement with a previous study (Li et al., 2013). Li et al. (2013) show that in the Bay of Bengal, climatologically post-monsoon season has higher low-level relative humidity than the pre-monsoon season. The higher relative humidity in the post-monsoon season is due to less dry air entrainment in the region as compared to the pre-monsoon season. Further, we find that the dew point depression at 850 hPa before the cyclone (averaged from day -7 to day -3) in both the basins is significantly lower than in the pre-monsoon season (Table S2). The correlation between the dew point depression at 850 hPa (averaged from day -7 to day -2) and the atmospheric temperature anomalies (850 hPa) is (r = -0.15) in the Arabian Sea and ($r = 0.14$) in the Bay of Bengal. This shows that in the Arabian Sea, the correlation is weak as compared to the pre-monsoon season. Despite a weaker correlation, it is statistically significant at 95% confidence level. As discussed earlier, a negative correlation indicates that with the increase in the dew point depression the atmosphere becomes more drier leading to an increase in evaporative cooling. In the Arabian Sea, since the lower atmosphere is moister (relative humidity = 62.97% and dew point depression = 7.05 K) in the post-monsoon season than the pre-monsoon season, it results in lesser evaporative cooling in the former season. This reduced evaporative cooling results in less negative temperature anomalies in the post-monsoon season (Figure 6a). In the Bay of Bengal, no evaporative cooling (~0°C temperature anomalies at 850 hPa) is observed at the 850 hPa (Figure 6b) and the role of dew point depression is insignificant as shown by weak positive correlation (r = 0.14). Thus, a drier lower atmosphere in the pre-monsoon season as compared to the post-monsoon season leads to higher evaporative cooling in the former season than the latter season. The evaporative cooling in the low levels observed for the north Indian Ocean cyclones is similar to cyclones in other basins (Rodgers et al., 1998; Zhang et al., 2002).

1. **Discussion**

In this study, we have analyzed the contrasting ocean-atmosphere interactions and upper atmospheric response to the north Indian Ocean cyclones during the

pre-monsoon and post-monsoon seasons for the period 1982–2019. We find that the oceanic response to cyclones in the Arabian Sea and the Bay of Bengal is different in the two cyclone seasons. Enhanced cyclone-induced SST cooling of magnitude 1.2°C in the Arabian Sea and 1.1°C in the Bay of Bengal is observed. However, during the post-monsoon season, the cyclone-induced SST cooling is significantly less than the pre-monsoon season in both basins. This is in line with previous studies, which show that this contrasting cyclone-induced SST cooling during the two seasons is associated with the ocean surface and sub-surface characteristics. In the post-monsoon due to the presence of thermal stratification in the Arabian Sea and haline stratification in the Bay of Bengal, the cyclone-induced SST cooling is weaker than the pre-monsoon season.

We find that, along with the ocean, the atmospheric response to the cyclones in the two seasons is also different from each other (Figure 8). During the pre-monsoon season, anomalous large cyclone-induced upper-level atmospheric warming of magnitude 3-4°C is observed. On the contrary, during the post-monsoon season, the cyclone-induced upper-level warming is about 1°C, which is significantly smaller than the pre-monsoon season. This contrasting response of the atmosphere to cyclones is due to the contrasting ocean-atmosphere coupled interaction in the two seasons. During the pre-monsoon season, higher pre-cyclone SSTs coupled with higher moisture disequilibrium between the ocean surface and near-surface and stronger wind forcing during cyclones enhance the latent heat flux exchange between the ocean and the atmosphere. Enhanced latent heat flux transfer from the ocean to the atmosphere leads to the anomalous higher moisture content in the lower levels of the atmosphere. This low-level anomalous high moisture is then transported by the secondary circulation within the cyclone and intense updrafts leading to enhanced convection, which in turn releases a large amount of latent heat of condensation at the upper levels. This leads to anomalous large upper-level warming during cyclones. On the other hand, during the post-monsoon season, lower SSTs as compared to the pre-monsoon season, coupled with weaker moisture disequilibrium and wind forcing during cyclones leads to a weak latent heat flux exchange between the ocean and the atmosphere. As a result, the convection during cyclones is weaker than in the pre-monsoon season. This leads to weak anomalous upper-level warming during the post-monsoon season cyclones. Earlier studies in other basins show that the processes governing the latent heating within the cloud of cyclones vary with height (Rodgers et al., 1998; Zhang et al., 2002). However, such analysis for the north Indian Ocean cyclones is out of the scope of this study and will be carried out in the future.

In sharp contrast to the anomalous cyclone-induced warming in the upper-levels, anomalous cooling is observed in the lower levels. The low-level anomalous cooling in both basins is more pronounced in the pre-monsoon season than in the post-monsoon season. The drier lower atmosphere during the pre-monsoon season as compared to the post-monsoon season leads to enhanced evaporative cooling of the rain falling through the lower atmosphere in the former than the latter season. Higher evaporative cooling in the pre-monsoon season leads to

stronger anomalous cooling in this season in the lower levels. Das & Subba (1972) show that the rate of evaporative cooling beneath a precipitating cloud also depends on the rain droplets' size distribution and the rainfall intensity. This is because, from the principles of thermodynamics, smaller rain drops have a larger surface-to-volume ratio thus exposing greater surface area for evaporation. Ankur et al. (2020) show that cyclones in the Bay of Bengal have higher rain intensity as compared to the Arabian Sea. However, the seasonal variation in the cyclone rainfall intensity and its size distribution is not yet understood. Thus, the characteristics of cyclone-induced rainfall can also play a significant role in the contrasting low-level cooling in the two cyclone seasons which need to be explored in the future.

The cyclone-induced upper-level warming is significantly affected by the changes in the SST and the latent flux exchange. Liu & Zhu, (2020) show that the latent heat of condensation released by Cyclone Fani at the upper levels in the Bay of Bengal has significantly altered the position of South Asian High pressure location. This shows that the upper-level cyclone-induced warming can significantly alter the heat budget balance in the atmosphere, which can alter wind circulation. Further, the updrafts in the cumulonimbus clouds can be significantly affected by the changes in the entrainment air in the cloud, low-level forcing, and fractional dilution with the environment air (Ferrier & Houze, 1989). In addition, high aerosol concentrations and the amount of condensate in clouds also affect the intensity of updrafts in the clouds with stronger updrafts are observed during high aerosol loading and high condensate (Khain et al., 2005; Zhang et al., 2002). Hence, the dependence of updrafts in the north Indian Ocean cyclones on the above-discussed factors and its association with changing SSTs needs to be further studied in detail in the future. The latent heat release in the clouds of a cyclone is also directly dependent on the amount of condensation and rainfall rate, and it increases with the cyclone rainfall rate (Adler & Rodgers, 1977). The north Indian Ocean continues to warm at a rapid pace (Roxy et al., 2015, 2019). With the continued warming of the north Indian Ocean, climate models project an increase in the cyclone rain rate in this basin (Knutson et al., 2020; Walsh et al., 2016). It needs to be seen how the latent heat release within the cyclone and upper-atmospheric warming will change in response to increasing SSTs and changing cyclone rain rates in the future.

Acknowledgments

The authors are grateful to Naresh Ganeshi from IITM, Pune, for assisting in the coding for plotting some of the figures. We thank Juby Aleyas Koll for preparing the schematic illustration for Figure 8.

Funding Information

None

Conflict of Interest

The authors declare no conflicts of interest relevant to this study.

Data Availability Statement

The cyclone data is obtained from JTWC as archived in the IBTrACS dataset and is available at https://www.ncdc.noaa.gov/ibtracs/ website. Various atmospheric variables used in the study are obtained from ERA5 reanalysis dataset and is available at https://www.ecmwf.int/en/forecasts/datasets/reanalysis-datasets/era5 website. SST data is obtained from NOAA OISST dataset and is available at https://psl.noaa.gov/data/gridded/data.noaa.oisst.v2.highres.html website.

References

Aberson, S. D., Zhang, J. A., & Ocasio, K. N. (2017). An extreme event in the eyewall of Hurricane Felix on 2 September 2007. *Monthly Weather Review*, *145*(6), 2083–2092. https://doi.org/10.1175/MWR-D-16-0364.1Adler, R. F. R. F., & Rodgers, E. B. E. B. (1977). Satellite-Observed Latent Heat Release in a Tropical Cyclone. *Monthly Weather Review*, *105*(8). https://doi.org/10.1175/1520-0493(1977)105<0956:SOLHRI>2.0.CO;2Ankur, K., Busireddy, N. K. R., Osuri, K. K., & Niyogi, D. (2020). On the relationship between intensity changes and rainfall distribution in tropical cyclones over the North Indian Ocean. *International Journal of Climatology*, *40*(4), 2015–2025. https://doi.org/10.1002/joc.6315Bao, J.-W. W., Wilczak, J. M., Choi, J.-K. K., & Kantha, L. H. (2000). Numerical simulations of air-sea interaction under high wind conditions using a coupled model: A study of Hurricane development. *Monthly Weather Review*, *128*(7 I), 2190–2210. https://doi.org/10.1175/1520-0493(2000)128<2190:NSOASI>2.0.CO;2Bender, M. A., & Ginis, I. (2000). Real-case simulations of hurricane-ocean interaction using a high-resolution coupled model: Effects on hurricane intensity. *Monthly Weather Review*, *128*(4), 917–946. https://doi.org/10.1175/1520-0493(2000)128<0917:RCSOHO>2.0.CO;2Black, R. A., Bluestein, H. B., & Black, M. L. (1994). Unusually Strong Vertical Motions in a Caribbean Hurricane. *Monthly Weather Review*, *122*(12), 2722–2739. https://doi.org/10.1175/1520-0493(1994)122<2722:usvmia>2.0.co;2Black, R. A., Heymsfield, G. M., & Hallett, J. (2003). Extra large particle images at 12 km in a hurricane eyewall: Evidence of high-altitude supercooled water? *Geophysical Research Letters*, *30*(21), 2124. https://doi.org/10.1029/2003GL017864Braun, S. A. (2002). A Cloud-Resolving Simulation of Hurricane Bob (1991): Storm Structure and Eyewall Buoyancy. *Monthly Weather Review*, *130*(6), 1573–1592. https://doi.org/10.1175/1520-0493(2002)130Chen, H., & Zhang, D. L. (2013). On the Rapid Intensification of Hurricane Wilma (2005). Part II: Convective Bursts and the Upper-Level Warm Core. *Journal of the Atmospheric Sciences*, *70*(1), 146–162. https://doi.org/10.1175/JAS-D-12-062.1Cione, J. J., & Uhlhorn, E. W. (2003). Sea Surface Temperature Variability in Hurricanes: Implications with Respect to Intensity Change. *Monthly Weather Review*, *131*(8), 1783–1796. https://doi.org/10.1175//2562.1Cione, J. J., & Uhlhorn, E. W. (2003). Sea surface temperature variability in hurricanes: Implications with respect to intensity change. *Monthly Weather Review*,

131(8 PART 2), 1783–1796. https://doi.org/10.1175//2562.1Cione, J. J., Kalina, E. A., Zhang, J. A., & Uhlhorn, E. W. (2013). Observations of Air–Sea Interaction and Intensity Change in Hurricanes. *Monthly Weather Review*, *141*(7), 2368–2382. https://doi.org/10.1175/MWR-D-12-00070.1Das, P., & Subba R.M.C. (1972). The unsaturated downdraft. *Indian Journal of Meteorological Geophysics*, *23*.Demaria, M., & Kaplan, J. (1994). Sea Surface Temperature and the Maximum Intensity of Atlantic Tropical Cyclones. *Journal of Climate*, *7*(9), 1324–1334. https://doi.org/10.1175/1520-0442(1994)007<1324:sstatm>2.0.co;2Durden, S. L. (2013). Observed Tropical Cyclone Eye Thermal Anomaly Profiles Extending above 300 hPa. *Monthly Weather Review*, *141*(12), 4256–4268. https://doi.org/10.1175/MWR-D-13-00021.1Eastin, M. D., Gray, W. M., & Black, P. G. (2005). Buoyancy of Convective Vertical Motions in the Inner Core of Intense Hurricanes. Part I: General Statistics. *Monthly Weather Review*, *133*(1), 188–208. https://doi.org/10.1175/MWR-2848.1Emanuel, K. A. A. An air-sea interaction theory for tropical cyclones. Part I: steady-state maintenance., 43 Journal of the Atmospheric Sciences § (1986). American Meteorological Society. https://doi.org/10.1175/1520-0469(1986)0432.0.CO;2Fairall, C. W., Bradley, E. F., Hare, J. E., Grachev, A. A., & Edson, J. B. (2003). Bulk Parameterization of Air-Sea Fluxes: Updates and Verification for the COARE Algorithm. *Journal of Climate*, *16*(4), 571–591.Ferrier, B. S., & Houze, R. A. (1989). One-dimensional time-dependent modeling of GATE cumulonimbus convection. *Journal of the Atmospheric Sciences*, *46*(3), 330–352. https://doi.org/10.1175/1520-0469(1989)046<0330:ODTDMO>2.0.CO;2Frank, W. M. (1977). The Structure and Energetics of the Tropical Cyclone II. Dynamics and Energetics. *Monthly Weather Review*, *105*(9), 1136–1150. https://doi.org/10.1175/1520-0493(1977)105<1136:tsaeot>2.0.co;2Gao, S., Zhai, S., Chiu, L. S., & Xia, D. (2016). Satellite air-sea enthalpy flux and intensity change of tropical cyclones over the western North Pacific. *Journal of Applied Meteorology and Climatology*, *55*(2), 425–444. https://doi.org/10.1175/JAMC-D-15-0171.1Gao, S., Chen, B., Li, T., Wu, N., & Deng, W. (2017). AIRS-observed warm core structures of tropical cyclones over the western North Pacific. *Dynamics of Atmospheres and Oceans*, *77*, 100–106. https://doi.org/10.1016/j.dynatmoce.2016.12.001Gao, S., Zhai, S., Chen, B., & Li, T. (2017). Water Budget and Intensity Change of Tropical Cyclones over the Western North Pacific. *Monthly Weather Review*, *145*(8). https://doi.org/10.1175/MWR-D-17-0033.1Gao, S., Jia, S., Wan, Y., Li, T., Zhai, S., & Shen, X. (2019). The role of latent heat flux in tropical cyclogenesis over the Western North Pacific: Comparison of developing versus non-developing disturbances. *Journal of Marine Science and Engineering*, *7*(2), 28. https://doi.org/10.3390/jmse7020028Hack, J. J. J., & Schubert, W. H. W. H. (1986). Nonlinear Response of Atmospheric Vortices to Heating by Organized Cumulus Convection. *Journal of Atmospheric Sciences*, *43*(15). https://doi.org/10.1175/1520-0469(1986)043<1559:NROAVT>2.0.CO;2Hersbach, H., Bell, B., Berrisford, P., Hirahara, S., Horányi, A., Muñoz-Sabater, J., et al. (2020). The ERA5 global reanalysis. *Quarterly Journal of the Royal Meteorological Society*, *146*(September

2019), 1–51. https://doi.org/10.1002/qj.3803Hirschberg, P. A. ., & Fritsch, J. M. (1993). On Understanding Height Tendency. *Monthly Weather Review*, *121*(9). https://doi.org/10.1175/1520-0493(1993)121<2646:OUHT>2.0.CO;2Houze, R. A. (2010, February). Clouds in tropical cyclones. *Monthly Weather Review*. https://doi.org/10.1175/2009MWR2989.1Houze, R. A., Lee, W. C., & Bell, M. M. (2009). Convective Contribution to the Genesis of Hurricane Ophelia (2005). *Monthly Weather Review*, *137*(9), 2778–2800. https://doi.org/10.1175/2009MWR2727.1Hu, X., Li, G. L., Zhang, C., & Yan, W. (2019). PRECIPITATION and LATENT HEATING PROPERTIES of TROPICAL CYCLONE in the NORTHWEST PACIFIC MEASURED by GPM DPR and HIMAWARI-8. In *International Archives of the Photogrammetry, Remote Sensing and Spatial Information Sciences - ISPRS Archives* (Vol. 42, pp. 77–82). International Society for Photogrammetry and Remote Sensing. https://doi.org/10.5194/isprs-archives-XLII-3-W9-77-2019Jaimes, B., Shay, L. K., & Uhlhorn, E. W. (2015). Enthalpy and momentum fluxes during hurricane earl relative to underlying ocean features. *Monthly Weather Review*, *143*(1), 111–131. https://doi.org/10.1175/MWR-D-13-00277.1Jaimes de la Cruz, B. ., Shay, L. K. ., Wadler, J. B. ., & Rudzin, J. E. (2021). On the Hyperbolicity of the Bulk Air–Sea Heat Flux Functions: Insights into the Efficiency of Air–Sea Moisture Disequilibrium for Tropical Cyclone Intensification. *Monthly Weather Review*, *149*(5), 1517–1534. https://doi.org/10.1175/MWR-D-20-0324.1Jorgensen, D. P. (1984). Mesoscale and Convective-Scale Characteristics of Mature Hurricanes. Part II. Inner Core Structure of Hurricane Allen (1980). *Journal of Atmospheric Sciences*, *41*(8). https://doi.org/10.1175/1520-0469(1984)041<1287:MACSCO>2.0.CO;2Kaplan, J., & DeMaria, M. (2003). Large-scale characteristics of rapidly intensifying tropical cyclones in the North Atlantic basin. *Weather and Forecasting*, *18*(6), 1093–1108. https://doi.org/10.1175/1520-0434(2003)018<1093:LCORIT>2.0.CO;2Khain, A., Rosenfeld, D., & Pokrovsky, A. (2005). Aerosol impact on the dynamics and microphysics of deep convective clouds. *Quarterly Journal of the Royal Meteorological Society*, *131*(611), 2639–2663. https://doi.org/10.1256/QJ.04.62Knapp, K. R., Kruk, M. C., Levinson, D. H., Diamond, H. J., Neumann, C. J., Kenneth R. Knapp, et al. (2010). The International Best Track Archive for Climate Stewardship (IBTrACS). *Bulletin of the American Meteorological Society*, *91*(3), 363–376. https://doi.org/10.1175/2009BAMS2755.1Knutson, T., Camargo, S. J., Chan, J. C. L. L., Emanuel, K., Ho, C.-H. H., Kossin, J., et al. (2020). Tropical cyclones and climate change assessment: Part2: projected response to anthropogenic warming. *Bulletin of the American Meteorological Society*, *101*(3), E303–E322. https://doi.org/10.1175/BAMS-D-18-0189.1Krishna, V. V. ., Murty, V. S. N. ., Sarma, M. S. S. ., & Sastry, J. S. (1993). Thermal response of upper layeys of bay of bengal to forcing of a severe cyclonic storm. *Indian Journal of Geo-Marine Sciences*, *22*(1).Kuo, H. L. (1965). On Formation and Intensification of Tropical Cyclones Through Latent Heat Release by Cumulus Convection. *Journal of the Atmospheric Sciences*, *22*(1), 40–63. https://doi.org/10.1175/1520-0469(1965)022<0040:ofaiot>2.0.co;2Lau, K. M. ., & Chan, P. H. (1986).

Aspects of the 40–50 Day Oscillation during the Northern Summer as Inferred from Outgoing Longwave Radiation. *Monthly Weather Review*, *114*(7), 1354–1367.Lawrence, M. G. (2005). The Relationship between Relative Humidity and the Dewpoint Temperature in Moist Air: A Simple Conversion and Applications. *Bulletin of the American Meteorological Society*, *86*(2), 225–234. https://doi.org/10.1175/BAMS-86-2-225Li, W. (2004). Modelling air-sea fluxes during a western Pacific typhoon: Role of sea spray. *Advances in Atmospheric Sciences*, *21*(2), 269–276. https://doi.org/10.1007/BF02915713Li, Y., Han, W., Ravichandran, M., Wang, W., Shinoda, T., & Lee, T. (2017). Bay of Bengal salinity stratification and Indian summer monsoon intraseasonal oscillation: 1. Intraseasonal variability and causes. *Journal of Geophysical Research: Oceans*, *122*(5), 4291–4311. Retrieved from https://agupubs.onlinelibrary.wiley.com/doi/abs/10.1002/2017JC012691Li, Z., Yu, W., Li, T., Murty, V. S. N., Tangang, F., Centre, R., et al. (2013). Bimodal character of cyclone climatology in the bay of bengal modulated by monsoon seasonal cycle. *Journal of Climate*, *26*(3), 1033–1046. https://doi.org/10.1175/JCLI-D-11-00627.1Lin, I. I., Chen, C. H., Pun, I. F., Liu, W. T., & Wu, C. C. (2009). Warm ocean anomaly, air sea fluxes, and the rapid intensification of tropical cyclone Nargis (2008). *Geophysical Research Letters*, *36*(3), 2–6. https://doi.org/10.1029/2008GL035815Liu, B., & Zhu, C. (2020). Boosting Effect of Tropical Cyclone "Fani" on the Onset of the South China Sea Summer Monsoon in 2019. *Journal of Geophysical Research: Atmospheres*, *125*(4), 1–16. https://doi.org/10.1029/2019JD031891Lloyd, I. D., & Vecchi, G. A. (2011). Observational evidence for oceanic controls on hurricane intensity. *Journal of Climate*, *24*(4), 1138–1153. https://doi.org/10.1175/2010JCLI3763.1Lord, S. J., Willoughby, H. E., & Piotrowicz, J. M. (1984). Role of a parameterized ice-phase microphysics in an axisymmetric, nonhydrostatic tropical cyclone model. *Journal of the Atmospheric Sciences*, *41*(19), 2836–2848. https://doi.org/10.1175/1520-0469(1984)041<2836:ROAPIP>2.0.CO;2Lucas, C., Zipser, E. J., & Lemone, M. A. (1994). Vertical Velocity in Oceanic Convection off Tropical Australia. *Journal of Atmospheric Sciences*, *51*(21), 3183–3193. https://doi.org/10.1175/1520-0469(1994)051<3183:VVIOCO>2.0.CO;2Malakar, P., Kesarkar, A. P., Bhate, J. N., Singh, V., & Deshamukhya, A. (2020). Comparison of Reanalysis Data Sets to Comprehend the Evolution of Tropical Cyclones Over North Indian Ocean. *Earth and Space Science*, *7*(2). https://doi.org/10.1029/2019EA000978Murthy, V. S., & Boos, W. R. (2018). Role of Surface Enthalpy Fluxes in Idealized Simulations of Tropical Depression Spinup. *Journal of the Atmospheric Sciences*, *75*(6), 1811–1831. https://doi.org/10.1175/JAS-D-17-0119.1Neetu, S., Lengaigne, M., Vincent, E. M., Vialard, J. J., Madec, G., Samson, G., et al. (2012). Influence of upper-ocean stratification on tropical cyclone-induced surface cooling in the Bay of Bengal. *Journal of Geophysical Research: Oceans*, *117*(12), 1–19. https://doi.org/10.1029/2012JC008433Nolan, D. S., Moon, Y., & Stern, D. P. (2007). Tropical Cyclone Intensification from Asymmetric Convection: Energetics and Efficiency. *Journal of the Atmospheric Sciences*, *64*(10), 3377–3405. https://doi.org/10.1175/JAS3988.1Nolan, D. S., Miyamoto, Y., Wu,

S. N., & Soden, B. J. (2019). On the Correlation between Total Condensate and Moist Heating in Tropical Cyclones and Applications for Diagnosing Intensity. *Monthly Weather Review*, *147*(10), 3759–3784. https://doi.org/10.1175/MWR-D-19-0010.1Ooyama, K. K. V. (1969). Numerical simulation of the life cycle of tropical cyclones. *Journal of Atmospheric Sciences*, *26*(1), 3–40. https://doi.org/10.1175/1520-0469(1969)026<0003:nsotlc>2.0.co;2Pokhrel, S., Dutta, U., Rahaman, H., Chaudhari, H., Hazra, A., Saha, S. K., & Veeranjaneyulu, C. (2020). Evaluation of Different Heat Flux Products Over the Tropical Indian Ocean. *Earth and Space Science*, *7*(6), e2019EA000988. https://doi.org/10.1029/2019EA000988Rao, R. (1987). analysis on the thermal response of the upper Bay of Bengal to the forcing of pre-monsoon cyclonic storm and summer monsoonal onset during MONEX-. *Mausam*, *11*, 1987. Retrieved from https://scholar.google.com/scholar?hl=en&as_sdt=0,5&q=Rao,+R.+R.+(1987),+Further+analysis+on monsoon+cyclonic+storm+and+summer+monsoon+onset+during+MONEX-79,+Mausam,+38(2),+147–156.Reynolds, R. W., Smith, T. M., Liu, C., Chelton, D. B., Casey, K. S., & Schlax, M. G. (2007). Daily High-Resolution-Blended Analyses for Sea Surface Temperature. *Journal of Climate*, *20*(22), 5473–5496. https://doi.org/10.1175/2007JCLI1824.1Rodgers, E., Olson, W., Halverson, J., Simpson, J., & Pierce, H. (2000). Environmental forcing of supertyphoon Paka's (1997) latent heat structure. *Journal of Applied Meteorology*, *39*(12 PART 1), 1983–2006. https://doi.org/10.1175/1520-0450(2001)040<1983:efosps>2.0.co;2Rodgers, E. B. ., Olson, W. S., Karyampudi, V. M., & Pierce, H. F. (1998). Satellite-Derived Latent Heating Distribution and Environmental Influences in Hurricane Opal (1995). *Monthly Weather Review*, *126*(5), 1229–1247.Rogers, R., Reasor, P., & Lorsolo, S. (2013). Airborne Doppler Observations of the Inner-Core Structural Differences between Intensifying and Steady-State Tropical Cyclones. *Monthly Weather Review*, *141*(9), 2970–2991. https://doi.org/10.1175/MWR-D-12-00357.1Rogers, R. F. ., Reasor, P. D., & Zhang, J. A. (2015). Multiscale structure and evolution of hurricane earl (2010) during rapid intensification. *Monthly Weather Review*, *143*(2), 536–562. https://doi.org/10.1175/MWR-D-14-00175.1Roxy, M., Tanimoto, Y., Preethi, • B, Terray, P., & Krishnan, • R. (2013). Intraseasonal SST-precipitation relationship and its spatial variability over the tropical summer monsoon region. *Climate Dynamics*, *41*(1), 45–61. https://doi.org/10.1007/s00382-012-1547-1Roxy, M. K., Dasgupta, P., McPhaden, M. J., Suematsu, T., Zhang, C., & Kim, D. (2019). Twofold expansion of the Indo-Pacific warm pool warps the MJO life cycle. *Nature*, *575*(7784), 647–651. https://doi.org/10.1038/s41586-019-1764-4Roxy, Mathew Koll, Ritika, K., Terray, P., Murtugudde, R., Ashok, K., & Goswami, B. N. (2015). Drying of Indian subcontinent by rapid Indian ocean warming and a weakening land-sea thermal gradient. *Nature Communications*, *6*(May), 1–10. https://doi.org/10.1038/ncomms8423Schade, L. R. (2000). Tropical cyclone intensity and sea surface temperature. *Journal of the Atmospheric Sciences*, *57*(18), 3122–3130. https://doi.org/10.1175/1520-0469(2000)057<3122:TCIASS>2.0.CO;2Schade, L. R., & Emanuel, K. A. (1999). The ocean's effect on the intensity of tropical cyclones: Re-

sults from a simple coupled atmosphere-ocean model. *Journal of the Atmospheric Sciences*, *56*(4), 642–651. https://doi.org/10.1175/1520-0469(1999)056<0642:TOSEOT>2.0.CO;2Schubert, W. H., & Hack, J. J. (1982). Inertial stability and tropical cyclone development. *Journal of the Atmospheric Sciences*, *39*(8), 1687–1697. https://doi.org/10.1175/1520-0469(1982)039<1687:ISATCD>2.0.CO;2Schubert, W. H., Rozoff, C. M., Vigh, J. L., McNoldy, B. D., & Kossin, J. P. (2007). On the distribution of subsidence in the hurricane eye. *Quarterly Journal of the Royal Meteorological Society*, *133*(624), 595–605. https://doi.org/10.1002/QJ.49Sengupta, D., Goddalehundi, B. R., & Anitha, D. S. (2008). Cyclone-induced mixing does not cool SST in thepost-monsoon north Bay of Bengal. *Atmospheric Science Letters*, *9*(October), 1–6. https://doi.org/10.1002/aslShay, L. K., & Uhlhorn, E. W. (2008). Loop Current Response to Hurricanes Isidore and Lili. *Monthly Weather Review*, *136*(9), 3248–3274. https://doi.org/10.1175/2007MWR2169.1Singh, V. K., & Roxy, M. K. (2022). A review of ocean-atmosphere interactions during tropical cyclones in the north Indian Ocean. *Earth-Science Reviews*, *226*, 103967. https://doi.org/10.1016/j.earscirev.2022.103967Subrahmanyam, B., Murty, V. S. N. N., Sharp, R. J., O'Brien, J. J., & O'Brien, J. J. (2005). Air-sea coupling during the tropical cyclones in the Indian Ocean: A case study using satellite observations. *Pure and Applied Geophysics*, *162*(8–9), 1643–1672. https://doi.org/10.1007/s00024-005-2687-6Takemi, T. (1999). Evaporation of Rain Falling Below a Cloud Base Through a Deep Atmospheric Boundary Layer Over an Arid Region. *Journal of the Meteorological Society of Japan*, *77*(2), 387–397.Thadathil, P., Muraleedharan, P. M., Rao, R. R., Somayajulu, Y. K., Reddy, G. V., & Revichandran, C. (2007). Observed seasonal variability of barrier layer in the Bay of Bengal. *Journal of Geophysical Research: Oceans*, *112*(2). https://doi.org/10.1029/2006JC003651Tong, H., Chandrasekar, V., Knupp, K. R., & Stalker, J. (1998). Multiparameter Radar Observations of Time Evolution of Convective Storms: Evaluation of Water Budgets and Latent Heating Rates. *Journal of Atmospheric and Oceanic Technology*, *15*(5), 1097–1109.Uhlhorn, E. W., & Shay, L. K. (2012). Loop Current Mixed Layer Energy Response to Hurricane Lili (2002). Part I: Observations. *Journal of Physical Oceanography*, *42*(3), 400–419. https://doi.org/10.1175/JPO-D-11-096.1Vigh, J. L., & Schubert, W. H. (2009). Rapid Development of the Tropical Cyclone Warm Core. *Journal of the Atmospheric Sciences*, *66*(11), 3335–3350. https://doi.org/10.1175/2009JAS3092.1Vinayachandran, P. N., Murty, V. S. N. N., Ramesh Babu, V., & Babu, V. R. (2002). Observations of barrier layer formation in the Bay of Bengal during summer monsoon. *Journal of Geophysical Research: Oceans*, *107*(12), 1–9. https://doi.org/10.1029/2001jc000831Vissa, N. K., Satyanarayana, A. N. V, & Kumar, B. P. (2013). Response of Upper Ocean and Impact of Barrier Layer on Sidr Cyclone Induced Sea Surface Cooling. *Ocean Sci. J*, *48*(3), 279–288. https://doi.org/10.1007/s12601-013-0026-xVissa, N. K. . K., Satyanarayana, A. N. V. V. ., Kumar, B. P., & Prasad Kumar, B. (2013). Intensity of tropical cyclones during pre- and post-monsoon seasons in relation to accumulated tropical cyclone heat potential over Bay of Bengal. *Natural Hazards*, *68*(2),

351–371. https://doi.org/10.1007/s11069-013-0625-yWalsh, K. J. E., Mcbride, J. L., Klotzbach, P. J., Balachandran, S., Camargo, S. J., Holland, G., et al. (2016). Tropical cyclones and climate change. *Wiley Interdisciplinary Reviews: Climate Change*, *7*(1), 65–89. https://doi.org/10.1002/wcc.371Wang, R., Xian, T., Wang, M., Chen, F., Yang, Y., Zhang, X., et al. (2019). Relationship between Extreme Precipitation and Temperature in Two Different Regions: The Tibetan Plateau and Middle-East China. *Journal of Meteorological Research 2019 33:5*, *33*(5), 870–884. https://doi.org/10.1007/S13351-019-8181-3Wang, S., & Toumi, R. (2021). Recent tropical cyclone changes inferred from ocean surface temperature cold wakes, *11*(1). https://doi.org/10.1038/s41598-021-01612-9Willoughby, H. E. (1998). Tropical Cyclone Eye Thermodynamics. *Monthly Weather Review*, *126*(12), 3053–3067. https://doi.org/10.1175/1520-0493(1998)126<3053:TCET>2.0.CO;2Wu, L., Wang, B., & Geng, S. (2005). Growing typhoon influence on east Asia. *Geophysical Research Letters*, *32*(18), 1–4. https://doi.org/10.1029/2005GL022937Wu, S. N., Soden, B. J., Miyamoto, Y., Nolan, D. S., & Buehler, S. A. (2021). Using Satellite Observations to Evaluate the Relationships between Ice Condensate, Latent Heat Release, and Tropical Cyclone Intensification in a Mesoscale Model. *Monthly Weather Review*, *149*(1), 113–129. https://doi.org/10.1175/MWR-D-19-0348.1Yanai, M., Esbensen, S., & Chu, J.-H. (1973). Determination of Bulk Properties of Tropical Cloud Clusters from Large-Scale Heat and Moisture Budgets. *Journal of the Atmospheric Sciences*, *30*(4), 611–627. https://doi.org/10.1175/1520-0469(1973)030<0611:dobpot>2.0.co;2Young, G. S., Ledvina, D. V., & Fairall, C. W. (1992). Influence of precipitating convection on the surface energy budget observed during a tropical ocean global atmosphere pilot cruise in the tropical western Pacific Ocean. *Journal of Geophysical Research: Oceans*, *97*(C6), 9595–9603. https://doi.org/10.1029/92JC00689Yu, Y., & Yao, X. (2011). Thermodynamic characteristics of tropical cyclones with rapid intensity change over the coastal waters of China, *25*(4). Retrieved from https://link.springer.com/article/10.1007/s13351-011-0407-yZawislak, J., & Zipser, E. J. (2014). Analysis of the Thermodynamic Properties of Developing and Nondeveloping Tropical Disturbances Using a Comprehensive Dropsonde Dataset. *Monthly Weather Review*, *142*(3), 1250–1264. https://doi.org/10.1175/MWR-D-13-00253.1Zhang, D.-L., Liu, Y., & Yau, M. K. (2002). A Multiscale Numerical Study of Hurricane Andrew (1992). Part V: Inner-Core Thermodynamics. *Monthly Weather Review*, *130*(11), 2745–2763.

	Arabian Sea Pre-monsoon
Latent heat flux anomaly (W m^{-2})	88.7
OLR anomaly (W m^{-2})	-108.8
Air temperature anomaly (300 hPa; °C)	3.74
Vertical velocity anomaly (averaged from 500-600 hPa; Pa s^{-1})	-0.76
Correlation between latent heat flux and OLR anomaly	-0.35
Correlation between OLR and air temperature anomaly (300 hPa)	-0.41
Correlation between OLR and vertical velocity anomaly (avg. from 500-600 hPa)	0.29

Table 1. Composite of anomalies of latent heat flux (W m^{-2}), OLR (W m^{-2}), air temperature (300 hPa, °C) and vertical velocity averaged from 500-600 hPa (Pa s^{-1}) on the day of cyclone (day 0) averaged over a 1°x1° area around the center of cyclone. Last three rows denote the correlation between the latent heat flux and OLR anomalies, the correlation between the OLR and air temperature anomalies (300 hPa) and the correlation between the vertical velocity averaged from 500-600 hPa and OLR anomaly respectively for the Arabian Sea and the Bay of Bengal during the pre-monsoon and post-monsoon seasons.

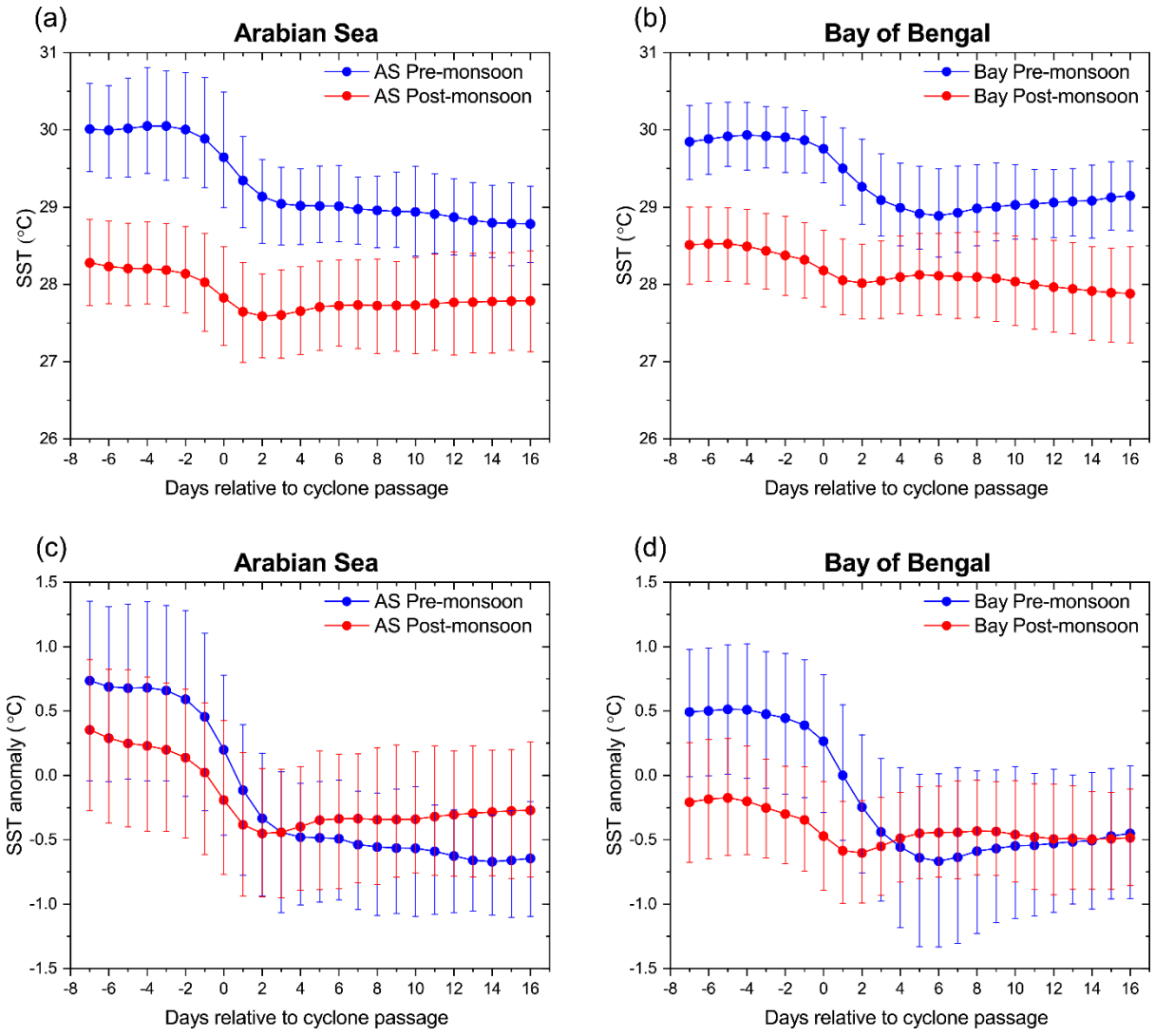

Figure 1. Composite evolution of SSTs (°C) from day -7 to day +16 with respect to the cyclone passage averaged over a 1°×1° area around the cyclone center for every cyclone location in the (a) Arabian Sea (b) Bay of Bengal during

the pre-monsoon (blue line) and the post-monsoon (red line) seasons for the period 1982–2019. Vertical bars long the line show the spread around the mean computed from the lower and upper quartiles. (c-d) same as (a-b) except for SST anomalies (°C).

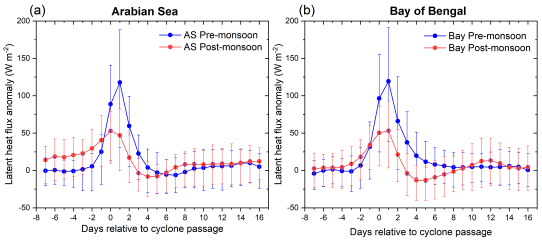

Figure 2. Composite evolution of latent heat flux anomaly (W m^{-2}) from day -7 to day +16 with respect to the cyclone passage averaged over a 1°×1° area around the cyclone center for every cyclone location in the (a) Arabian Sea (b) Bay of Bengal during the pre-monsoon (blue line) and post-monsoon (red line) seasons for the period 1982–2019. Vertical bars show the spread around the mean computed from the lower and upper quartiles.

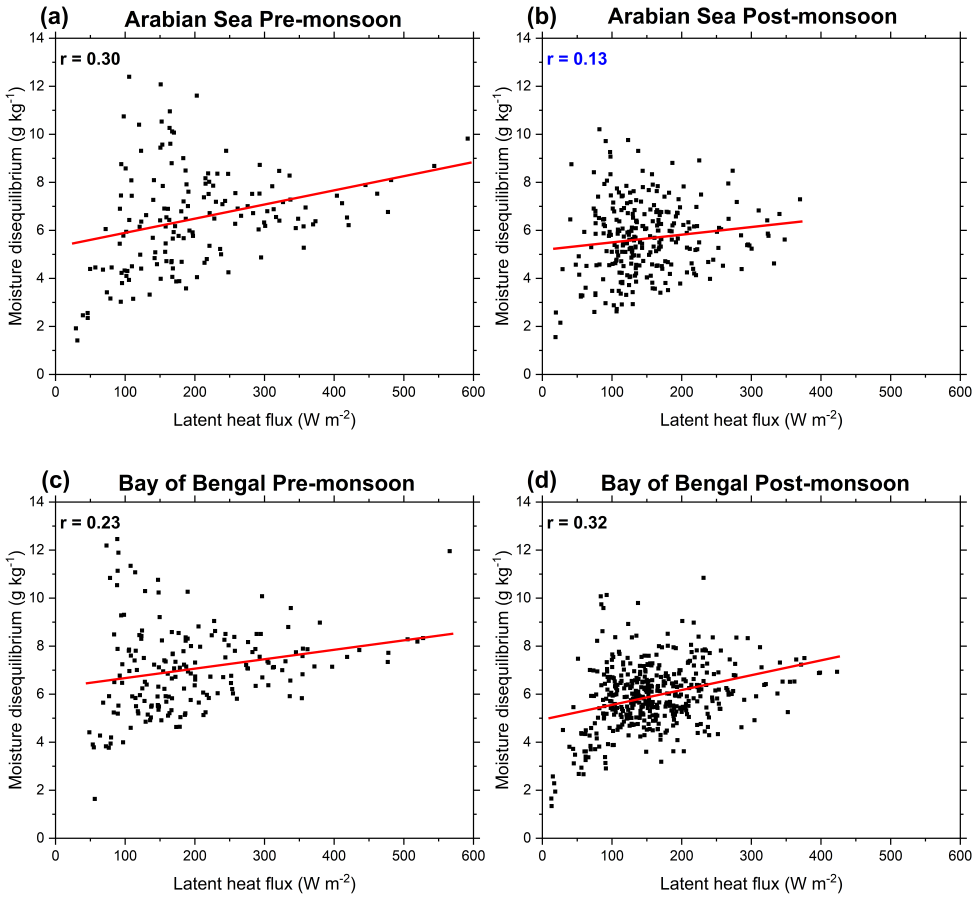

Figure 3. Scatterplot of latent heat flux (W m^{-2}) vs moisture disequilibrium (q_s-q_a , g kg^{-1}) on the day of cyclone (day 0) averaged over a 1°×1° area around the cyclone center for every cyclone location in the (a) Arabian Sea pre-monsoon season (b) Arabian Sea post-monsoon season (c) Bay of Bengal pre-monsoon season (d) Bay of Bengal post-monsoon season. The values in the top left corner of each panel shows the correlation between the latent heat flux and the moisture disequilibrium (q_s-q_a). The correlation coefficients shown in black are statistically significant at 99% confidence level and the correlation coefficient shown in blue is statistically significant at 95% confidence level.

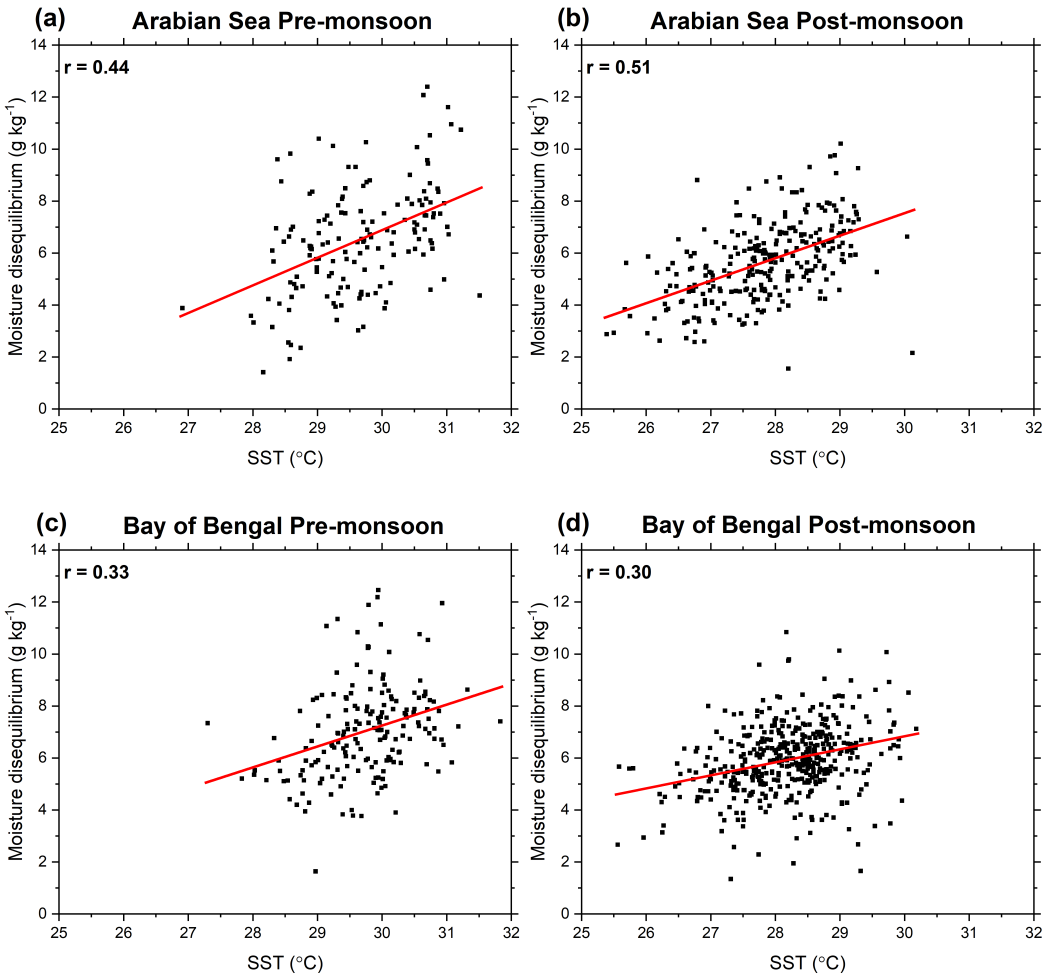

Figure 4. Scatterplot of SST (°C) vs moisture disequilibrium (q_s-q_a, g kg^{-1}) on the day of cyclone (day 0) averaged over a 1°×1° area around the cyclone center for every cyclone location in the (a) Arabian Sea pre-monsoon season (b) Arabian Sea post-monsoon season (c) Bay of Bengal pre-monsoon season (d) Bay of Bengal post-monsoon season. The values in the top left corner of each panel shows the correlation between the SST and the moisture disequilibrium. All the correlation coefficients are statistically significant at 99% confidence level.

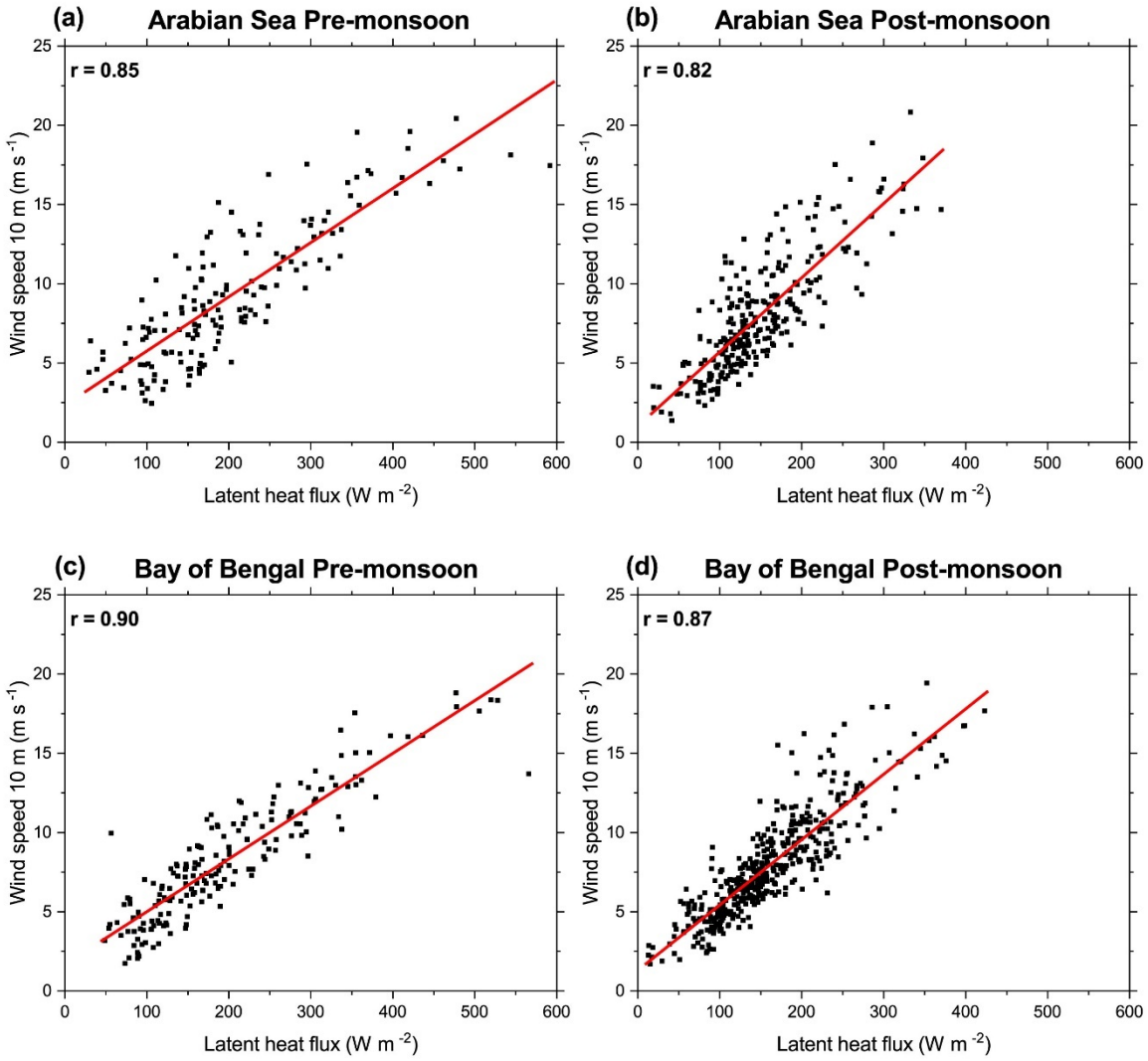

Figure 5. Scatterplot of latent heat flux (W m^{-2}) vs wind speed at 10 m (m s^{-1}) on the day of cyclone (day 0) averaged over a 1°×1° area around the cyclone center for every cyclone location in the (a) Arabian Sea pre-monsoon season (b) Arabian Sea post-monsoon season (c) Bay of Bengal pre-monsoon season (d) Bay of Bengal post-monsoon season. The values in the top left corner of each panel shows the correlation between the latent heat flux and the wind speed at 10 m. All the correlation coefficients are statistically significant at 99% confidence level.

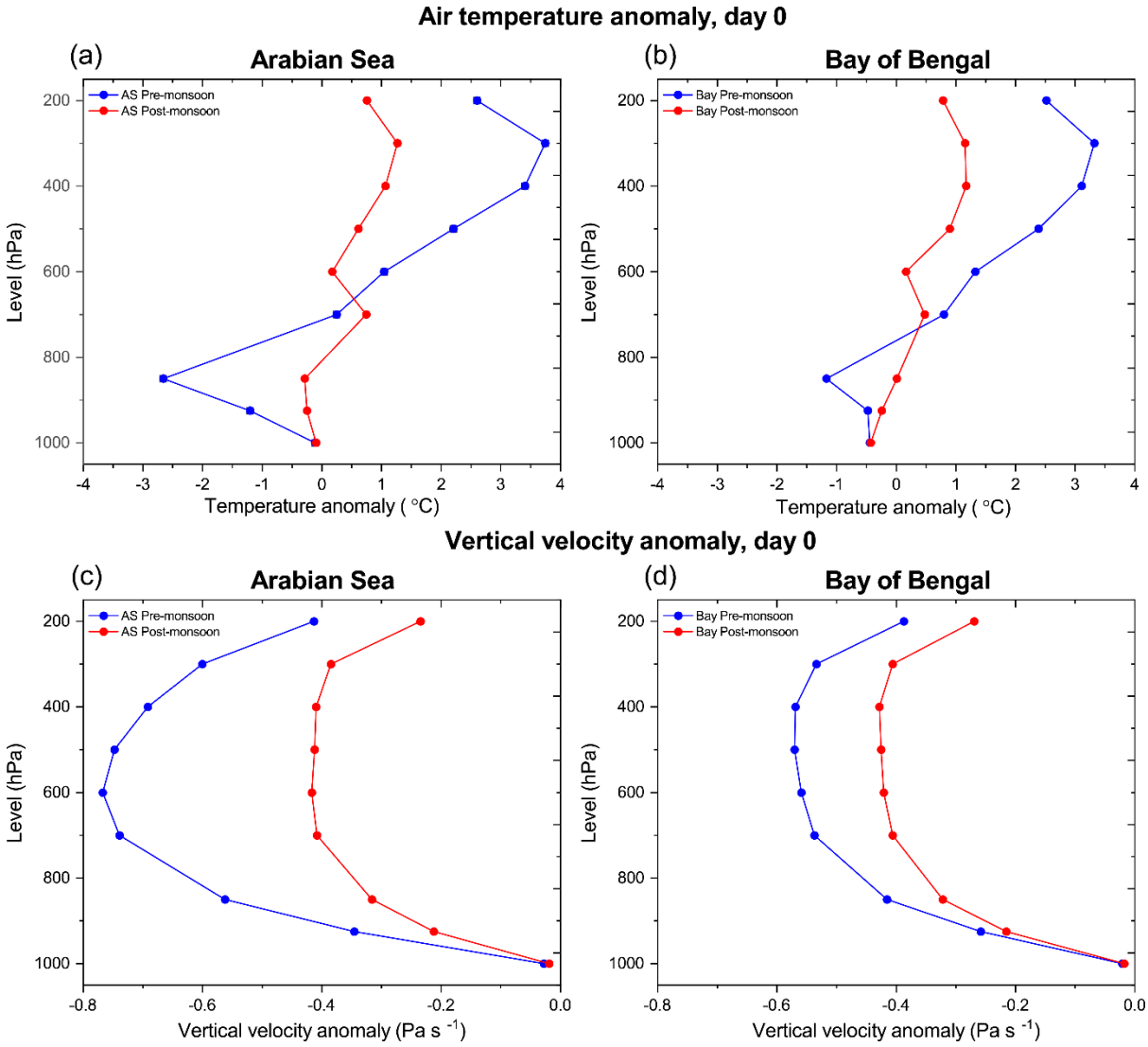

Figure 6. Mean vertical profile of (a-b) atmospheric temperature anomaly (°C) and (c-d) vertical velocity anomaly (negative values indicate updraft, Pa s^{-1}) during the day of cyclone (i.e at day 0) averaged over a 1°×1° area around the center of cyclone in the Arabian Sea and the Bay of Bengal during the pre-monsoon (blue line) and post-monsoon seasons (red line) for the period 1982–2019.

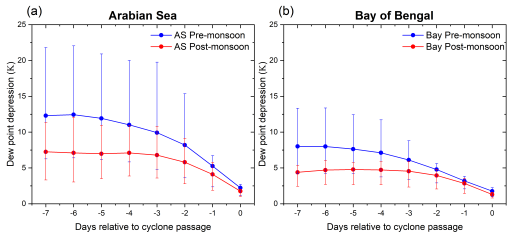

Figure 7. Composite of dew point depression (K) at 850 hPa from day -7 to day 0 averaged over a 1°×1° area around the center of cyclone from every cyclone location in the (a) Arabian Sea (b) Bay of Bengal during the pre-monsoon (blue line) and post-monsoon (red line) seasons for the period 1982–2019. Vertical bars show the spread around the mean computed from the lower and upper quartiles.

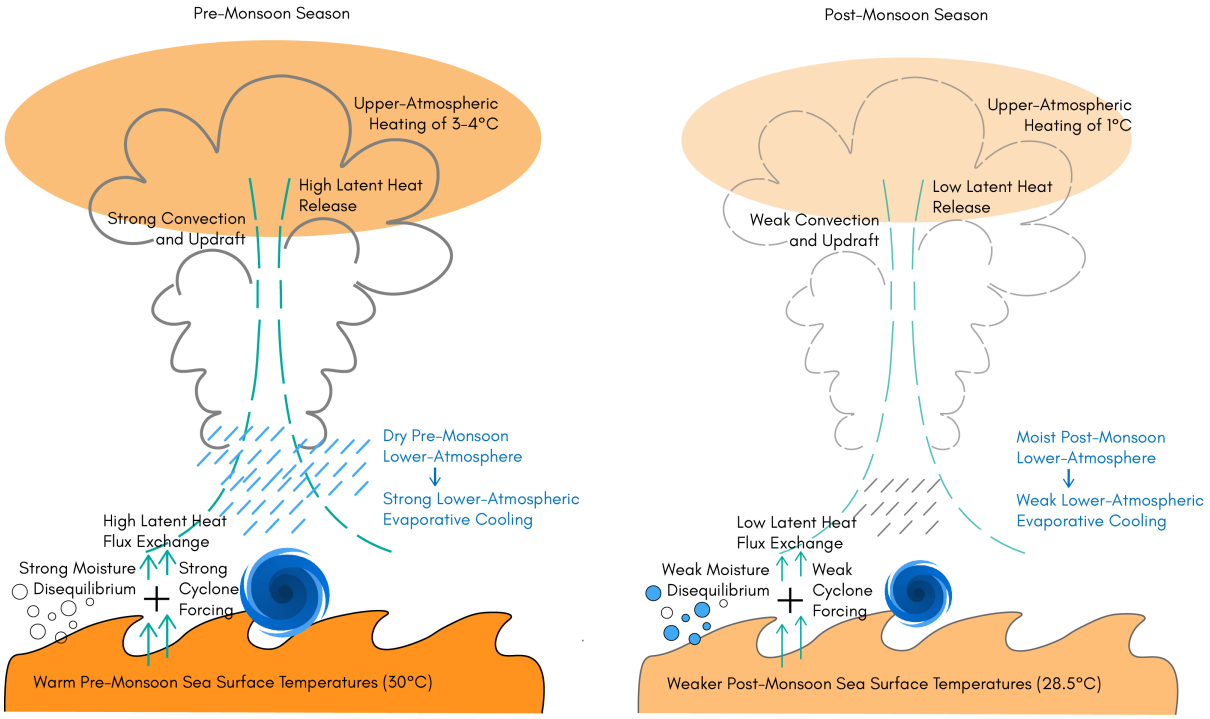

Figure 8. Schematic of the atmospheric response to cyclones in the north Indian Ocean during pre-monsoon and post-monsoon cyclone seasons. During the pre-monsoon season, warm sea surface temperatures (30°C), strong moisture disequilibrium, and a strong cyclone wind forcing lead to high latent heat flux exchange, enhancing the convection and updraft, resulting in high latent heat release and upper atmospheric heating (3–4°C). Dry lower-atmospheric conditions during the pre-monsoon leads to a strong evaporative cooling at this level as precipitation occurs. During the post-monsoon season, relatively weaker sea surface temperatures (28.5°C), weak moisture disequilibrium, and a weak cyclone wind forcing lead to low latent heat flux exchange, reducing the convection and updraft, resulting in low latent heat release and upper atmospheric heating (1°C). Moist lower-atmospheric conditions during the post-monsoon leads to a weak evaporative cooling at this level as precipitation occurs.